C.P. No. 883

C.P. No. 883

MINISTRY OF AVIATION

AERONAUTICAL RESEARCH COUNCIL

CURRENT PAPERS

A Study on the Running Times in Reflected Shock Tunnels

By

J. A. D. Ackroyd

LONDON: HER MAJESTY'S STATIONERY OFFICE

1967

EIGHT SHILLINGS NET

C.P. No. 883

January, 1965

A STUDY ON THE RUNNING TIMES IN REFLECTED SHOCK TUNNELS

by

J. A. D. ACKROYD
Department of Aeronautical Engineering,
Queen Mary College.

Communicated by Professor A. D. Young.

SUMMARY

The running time obtainable in a reflected shock tunnel is considered, particular attention being paid to the nature of the unsteady wave starting process in the nozzle. A range of initial conditions has been examined experimentally in a two-dimensional nozzle with a maximum efflux-to-throat area ratio of 100. An approximate analysis based on Chisnell's theory is shown to give reasonable agreement with the experimental results.

CONTENTS

Replaces A.R.C. 26 631

1. INTRODUCTION.

The shock tube and its derivative the hypersonic reflected shock tunnel are now firmly established as useful intermittent facilities for experiments on high speed, high stagnation enthalpy gas flows. They rely on a process by which the initially stationary test gas at room temperature is raised to a high temperature and a velocity imparted to it by one or more unsteady shock waves of predictable strength. The amount of test gas initially in the system is generally small; it follows that the duration of quasi-steady flow is short. Clearly, in such short duration hypersonic facilities it is important to know how far the need to simulate such flow parameters as Mach number, stagnation enthalpy and Reynolds number affects the duration of steady test flow.

The problem of the steady flow duration or running time obtainable in the simple shock tube for any given initial conditions is examined in reference 1. It is shown, for example, that the running time decreases with decreasing initial channel pressure. The dependence of running time on initial channel pressure is one example of the interrelationship between steady flow duration and flow simulation, the simulation parameter being in this case the Reynolds number.

The Mach number of the quasi-steady flow produced by the primary shock wave in the channel of the simple shock tube is always relatively low. To increase the test flow Mach number available a simple divergent nozzle can be fitted to the end of the shock tube channel. The quasi-steady flow of test gas produced in the shock tube channel expands to the required hypersonic flow Mach number on encountering the diverging section of the nozzle. The primary shock wave must, however, precede this expansion. Unfortunately, the interaction between this shock wave and the diverging section is such that the shock wave attenuates and a backward facing wave is formed behind the shock wave as it moves through the diverging section. A considerable amount of the test gas passes through this backward facing wave and arrives at the nozzle efflux with conditions appreciably modified by this wave. Provided that the backward facing wave does not grow to a sufficient strength such as to come to rest in the nozzle, it will eventually be swept through. The remaining test gas can then expand to the desired conditions unhindered by any further waves in the diverging section. However, the steady flow duration at the end of the nozzle is considerably reduced by the presence of the secondary wave system. The running time obtainable in this 'straight-through' type of hypersonic shock tunnel is discussed by Henshall and Gadd in reference 2.

Various physical configurations of the basic shock tube and nozzle combination have been examined in an attempt to alleviate the problem of the interaction of the shock wave with the area change associated with the divergence of the nozzle walls. The most successful of these configurations is that known as the reflected shock tunnel and is discussed in, for example, references 4 and 5.

In the reflected shock tunnel configuration the shock tube channel is terminated by a convergent-divergent nozzle. A second diaphragm is generally placed at the nozzle throat, allowing the nozzle and the working section to be evacuated to a much lower pressure than that in the channel. Consequently, the primary shock wave is entirely reflected on reaching the effectively closed

end of the channel. The reflected shock wave now moves through the oncoming test gas and passes into the expanded driver gas. The test gas is brought to rest and the pressure and temperature further raised by the reflected shock wave. The sudden increase in test gas pressure, due to the reflection of the shock wave at the end of the channel, is arranged to be sufficient to burst the nozzle diaphragm, whereupon the stagnant test gas begins to expand through the convergent-divergent nozzle to the required conditions. Again, in this configuration an unsteady wave system must precede this steady expansion through the nozzle. The unsteady wave system interacts with the diverging section of the nozzle but it has been found experimentally that, in this case, the starting waves generally pass rapidly through the nozzle. The reasons for this will become apparent later. However, relatively small values of steady flow duration (or running time) have occurred under certain conditions in the working sections of reflected shock tunnels.

To the author's knowledge, no satisfactory description has been produced of the wave starting processes in the nozzles of reflected shock tunnels. The analyses of sections 3 to 5 attempt to discuss this problem. It is argued that the unsteady wave system generated at the nozzle throat by the bursting of the nozzle diaphragm is similar to that in the simple shock tube with a heated driver gas and an area change at the diaphragm. The subsequent interaction of this unsteady wave system with the diverging walls of the nozzle is examined. Use is made of an analysis due to Chisnell[3] which examines the interaction of a shock wave with a variable area duct.

A description is given in section 6 of the small shock tube of the Queen Mary College hypersonics laboratory to which a convergent-divergent, two dimensional nozzle has been added. This apparatus has been used to investigate the nozzle starting process in reflected shock tunnels. Section 7 presents the experimental details.

2. THE STEADY FLOW DURATION AT THE NOZZLE THROAT OF A REFLECTED SHOCK TUNNEL AT TAILORING CONDITIONS.

In order to utilise all the high enthalpy compressed channel gas flow between the primary shock wave and the contact surface it is necessary to ensure that the primary shock wave, on reflection from the end of the channel and on meeting the contact surface, does not produce a further wave which moves back into the channel gas. The condition at which the channel gas remains undisturbed throughout the reflected shock wave-contact surface interaction is known as the tailored condition and is illustrated in the (x,t) plane of Figure 1. For the case of hydrogen driving into nitrogen, both gases being initially at room temperature, it has been shown[4] that the primary shock Mach number necessary to achieve the tailored conditions is approximately 6.0.

Once the nozzle diaphragm has burst the compressed stagnant channel gas expands through the nozzle throat and into the working section. Eventually, at some time t_R^* after primary shock-wave reflection, all the test gas in region 5 (see Fig. 1) will have passed through the nozzle throat. Holder and Schultz have shown in reference 5 that the steady flow duration, t_R^*,

at the nozzle throat at the tailored condition may be related to the running time available at the end of the channel, t_R, by the equation

$$\frac{t_R^*}{t_R} = 1 + \frac{1}{\left|\frac{u_2}{W_2}\right|+1}\left[\frac{u_2}{a_5}\left(\frac{\gamma_5+1}{2}\right)^{\alpha_5/2}\frac{A_D'}{A^*} - 1\right] \qquad 2.1$$

The ratio A_D'/A^* is the area ratio of channel to throat. The velocities u_2 and W_2 are respectively, the contact surface velocity and the velocity of the reflected shock wave, a_5 being the sound speed in region 5 behind this reflected wave (see Fig. 1).

Inserting the numerical values for the tailored condition for hydrogen driving into nitrogen and assuming that the ratio of A_D'/A^* is large, equation 2.1 gives

$$\frac{t_R^*}{t_R} \simeq 0.62\,\frac{A_D'}{A^*} \qquad 2.2$$

Equation 2.1 is derived directly from the steady flow continuity equation connecting conditions in region 5 (Fig. 1) and the nozzle throat and neglects viscous and real gas effects. However, we note that the flow through the nozzle throat must be initiated by an unsteady rarefaction wave generated by the bursting of the nozzle diaphragm. In the preceding statement we have assumed that a short delay occurs between primary shock wave reflection and the bursting of the diaphragm. As we shall argue in more detail later, the strength of this rarefaction wave will be weak for large values of A_D'/A^* and the wave will rapidly overtake the reflected shock wave. Consequently, the initial unsteadiness in the expansion to the nozzle throat may be neglected and equation 2.2 remains acceptable.

Holder and Schultz (loc. cit.) have examined the influence of real gas effects and have shown that if the flow is in equilibrium between region 5 and the throat, a better approximation to equation 2.1 is

$$\frac{t_R^*}{t_R} \simeq 0.8\,\frac{A_D'}{A^*} \qquad 2.3$$

There are a number of reasons why this duration of steady flow at the nozzle throat, t_R^*, is not obtainable in the reflected shock tunnel working section. For example, the reflected head of the rarefaction wave generated at the rupture of the main diaphragm may arrive at the end of the channel before all the reservoir gas at condition 5 has passed through the nozzle throat. Since the design of driver and channel to remove this defect is discussed in detail in reference 5 it will not be examined further here. A more serious difficulty arises from the wave system which precedes the steady expansion through the nozzle and here, although the full duration of steady flow may be achieved at the nozzle throat, the steady flow duration in the working section can be much less than t_R^*. This difficulty is discussed in more detail in the following sections.

It is noted that should an estimate of t_R^* be made using equations 2.1 to 2.3 it would be preferable to estimate first a value of t_R using the analysis given, say, in reference 1.

3. THE NOZZLE STARTING PROCESS.

On the reflection of the primary shock wave at the tailored condition from the virtually closed end of the channel we have a situation essentially similar to that of the simple shock tube with a heated driver gas. The high pressure, high enthalpy gas at the condition 5 (Fig. 2a) acts as the driving gas for the shock wave of velocity W_N^* (Mach number M_{SN}^*) formed close to the nozzle throat. We may also take account of the effect on the value of M_{SN}^* of the area change from channel to throat (A_D' to A^*, see Fig. 2b). Lukasiewicz[7] has shown that under these circumstances an unsteady rarefaction wave moves into the driver gas but is followed by a steady expansion of the driver gas through the area change. If the diaphragm pressure ratio is sufficiently high, the expanded driver gas may reach supersonic speed; then a second part of the unsteady rarefaction wave exists to provide the further expansion of the driver gas from sonic conditions (see Fig. 2b). If the area change from channel to throat is large, Lukasiewicz has shown that the section of the backward facing unsteady rarefaction wave which moves into region 5 will be weak and that most of the expansion process to sonic conditions is achieved through the steady expansion. This argument justifies the neglect of the effect of the unsteady rarefaction wave on the value of the throat running time, t_R^*, in the previous section.

Alpher and White[8] have also considered the original problem approached by Lukasiewicz (i.e. the simple shock tube problem incorporating an area reduction from driver to channel) and were able to show that this type of shock tube behaved as if it were a constant area shock tube with a diaphragm pressure ratio of g times the actual diaphragm pressure ratio and a speed of sound ratio of $g^{(\gamma-1)/2\gamma}$ times the actual speed of sound ratio, the value of γ being that of the driver gas. Graphs of g against area ratio for various values of γ may be found in reference 8. Consequently, in applying the channel-to-throat area change effect to the estimation of the throat shock Mach number, M_{SN}^*, it would appear to be necessary to multiply the speed of sound ratio across the nozzle diaphragm, A_{SN}, by the factor $g^{(\gamma_5-1)/2\gamma_5}$ and the actual diaphragm pressure ratio, P_{SN}, by g. Since γ_5 is close to unity, due to real gas effects (and typically g lies between 1 and 2) the factor $g^{(\gamma_5-1)/2\gamma_5}$ is close to unity and its effect on the actual speed of sound ratio may be neglected. Hence, the effective pressure ratio, $g\,P_{SN}$, may be related to the throat shock Mach number, M_{SN}^*, by the simple constant area shock tube equation, the results of which are plotted in Fig. 3. In obtaining all the curves of Fig. 3 real gas values of the parameters in region 5 have been used (see reference 6 and further data given in unpublished work by Bernstein). In an attempt to account for the imperfect nature of the nozzle gas behind the shock wave we have used the equilibrium real gas shock wave tables of Bernstein[6]. It has been assumed in all the calculations summarised in Fig. 3 that the gas at condition 5 expands at a frozen condition whilst the nozzle gas processed by the shock wave is either perfect or is a real gas in equilibrium. In the latter case the conditions in the nozzle gas behind the shock wave will depend upon the initial pressure in the nozzle p_N. Two values of p_N, namely 1 mm. Hg. and 0.01 mm. Hg., are used as examples in Fig. 3.

We now require to know how the interaction of the starting shock wave (initially of shock Mach number M_{SN}^* as determined above) with the area change along the nozzle modifies the speed of the starting shock wave.

Chisnell[3] has investigated the problem of a shock wave moving through an elementary area increase $\delta A'$. His model assumes a transmitted shock wave, an elementary interface and an elementary backward facing compression wave. He extends his analysis to the case of a finite area change by integrating the effects of the elementary area changes. He neglects any effects on the shock wave arising from the complex wave interactions which occur behind it and parts of which must overtake it. He shows that an approximate relationship exists between the shock Mach number, M_s, and the area A' such that

$$A'^{K}\left(M_s^2-1\right) = \text{const.} \qquad 3.1$$

(The index K depends upon the strength of the shock wave but for strong shock waves in diatomic gases is very close to 0.4.)

Chisnell is further able to show that for the case of a strong converging shock wave the multitude of elementary wave interactions which might overtake the shock wave later in its trajectory fortuitously cancel each other. In this particular case the results of Chisnell's analysis are in close agreement with the exact analysis of Guderley (see Ref. 3) for strong converging shock waves.

We shall therefore approximate the trajectory of the starting shock wave, M_{SN}, by applying the results of Chisnell's analysis to the continuous, unsteady interaction of the starting shock wave with the area change from A^* to, say, A' occurring at the nozzle efflux. We shall retain the approximation that $K=0.4$ since, in general, the starting shock wave is initially exceedingly strong and quite strong on emergence from the nozzle. Hence, we may write the relationship between the shock Mach number, M_{SN}, and the area A' from equation 3.1 as

$$\left.\begin{aligned} \bar{A}^{0.4} &= \frac{M_{SN}^{*2}-1}{M_{SN}^2-1}, \\ \bar{A} &= A'/A^*. \end{aligned}\right\} \qquad 3.2$$

It is seen from equation 3.2 that as the area ratio increases the value of the shock Mach number, M_{SN}, decreases.

Now, taking the area A' to be at a distance ξ from the nozzle throat, it follows that the time taken, t_s, for the starting shock wave to traverse the distance ξ is, from equation 3.2,

$$t_s = \frac{1}{a_N}\int_0^{\xi}\frac{d\xi}{\left[\bar{A}^{-0.4}\left(M_{SN}^{*2}-1\right)+1\right]^{1/2}}. \qquad 3.3$$

For any particular nozzle shape a relationship exists between the area ratio and the distance from the throat ξ. Hence, it may be possible to integrate equation 3.3 formally (see, for example, reference 13). However, difficulties may arise in evaluating the integral and it may be quicker to evaluate equation 3.3 numerically. For the case in which $\bar{A}$ is a linear function

of ξ the integral had to be evaluated to ten decimal places.

Besides the starting shock wave discussed above, there is also a contact surface formed, as shown in Fig. 2c., when the nozzle diaphragm ruptures. This contact surface represents the division between the expanded reservoir gas and the gas which initially occupied the nozzle. The contact surface will move through the nozzle at the local gas velocity. Referring to Fig. 2c, it is noted that there exists a region of continuously changing entropy (or contact region) between the starting shock wave and the contact surface. This contact region is suggested in Chisnell's model and is accounted for by the different values of entropy held by the various parts of the shocked nozzle gas which have each been processed by a shock wave of different strength. The various elements of this region will travel at the local gas velocity and thus the region always lies between the shock wave and the contact surface but increases in extent and strength (in terms of the overall density change through the region) as the starting shock wave moves through the nozzle.

Simple considerations of the nozzle starting process show that besides the starting shock wave, contact surface and contact region there exists a further backward facing wave*. Henshall and Gadd[2] have shown in the case of the 'straight-through' operation of the shock tunnel (where there is no throat) that this backward facing wave may be either a rarefaction wave or a shock wave. The backward facing wave must exist to match the unsteady conditions achieved by the starting shock wave and the steady isentropic expansion of the reservoir conditions from region 5 since in general the pressures and gas velocities obtained through these processes are not equal. The application of Chisnell's model to the discussion of the strength and nature of the backward facing wave is complicated by the presence of the contact surface in this particular case and also by the fact that in the Chisnell model the backward facing wave is composed of compression waves which are assumed not to coalesce. Furthermore, it is noted that the backward facing wave will also interact with the area change through which it is moving. Solutions to this type of problem of unsteady wave motion in established flows have, so far, met with little success (see reference 9).

4. THE 'STEADY' STATE MODEL.

An appeal has been made to the 'steady' state model shown in Fig. 4 to provide an estimate of the maximum strength the backward facing wave may possess for any particular values of $\bar{A}$ and $M_{S_N}^*$. If the backward facing wave is a shock wave, although growing in strength as it moves through the area change from A^* to A' as more elementary compression waves coalesce with it, it is at the stage of complete coalescence in the 'steady' state model. The velocities (in laboratory co-ordinates) of the completely coalesced backward facing shock waves computed from the 'steady' state model should, then, be always less than the velocities of the backward facing but not completely coalesced compression waves expected in practice. Hence, an upper limit to the backward facing wave trajectory through the nozzle (see Fig. 5) may be determined. However, in the case where the backward facing wave is a rarefaction wave we shall only use the 'steady' state model to demonstrate that, in fact, the wave is a rarefaction wave. The strength of this wave is of no interest to us; the head of the wave always travels at sonic speed

---

*Since this paper was prepared, Smith[15,16] has shown, by means of a complete characteristics solution of the nozzle starting process, that this backward facing wave is always a shock wave which interacts continuously with a backward facing rarefaction wave. For a more detailed examination of the strength and nature of this backward facing wave system, the reader is directed to Smith's

relative to the gas into which it is moving. Since the head of a backward facing rarefaction wave (or an elementary compression wave) achieves the highest velocity in being swept through the nozzle the trajectory of a backward facing shock wave should always lie between the upper limit of the always completely coalesced shock wave trajectory and the head of a rarefaction wave trajectory (see Fig. 5).

The method of calculation employed in the 'steady' state models examined has been simplified by assuming that for any values of M_{SN}^{*} and $\bar{A}$ the strength of the starting shock wave, M_{SN}, is given by Chisnell's analysis. This assumption will be justified later in section 8.

Referring to Fig. 4, knowing the value of M_{SN} for particular values of $\bar{A}$ and M_{SN}^{*}, then we know the value of the pressure ratio p_{5d}/p_{N}. The actual pressure ratio, p_{SN}, is known from Fig. 3 for the particular shock tunnel configuration. The value of g chosen here was appropriate to the shock tunnel configuration used in the present experimental investigation (section 6). Hence, the steady expansion pressure ratio, p_5/p_{5c}, is now only required in order to establish the strength and nature of the backward facing wave. Here we have neglected entirely the pressure decrease occurring through the weak rarefaction wave which moves into region 5 when the nozzle diaphragm bursts. Two methods have been used to compute the value of p_5/p_{5c}, the first being based on equilibrium values of this pressure ratio given by Bernstein[10] for nitrogen. However, experiments by Stollery and Townsend[11] indicate that, in fact, the gas may expand in equilibrium to approximately the nozzle throat position but thereafter the excitation states are 'frozen'. Consequently, for the second method equilibrium flow has been assumed from the reservoir state 5 to the nozzle throat, the gas parameters (p_5/p^{*}, a^{*}, γ^{*} etc.) at the nozzle throat being obtained from (unpublished) data by Bernstein. The subsequent expansion from the throat is treated as one dimensional steady 'frozen' flow.

The results of the two methods of calculation for the velocity of the wave in laboratory co-ordinates, W_{5c}, for values of $\bar{A}$ from 1 to 10^4 and values of M_{SN}^{*} from 6 to 20 are shown in Fig. 6a and 6b. The equilibrium flow calculations are shown in Fig. 6a and Fig. 6b relates to the frozen flow calculations. Both sets of curves indicate that for certain values of M_{SN}^{*} and $\bar{A}$ the backward facing wave (in fact, a shock wave) is brought to rest. Under these conditions the tunnel flow never starts.

In both Fig. 6a and 6b the upper curves (for $M_{SN}^{*} = 20$) represent trajectories of the heads of backward facing rarefaction waves. The remaining curves which fall below that for $M_{SN}^{*} = 20$ or diverge from it represent the cases where backward facing shock waves appear. Hence, in order to obtain the shortest possible starting time it is necessary to ensure that the backward facing wave is always a rarefaction wave. Fig. 6 suggests that it is necessary for M_{SN}^{*} to be high for the values of $\bar{A}$ usually employed in reflected shock tunnels.

5. THE RUNNING TIME IN THE WORKING SECTION OF A REFLECTED SHOCK TUNNEL.

The time taken, t_B, for the backward facing wave to be swept from the

nozzle throat ($\xi = 0$) to the nozzle efflux at $\bar{A}$ ($\xi = \xi_1$, say) is

$$t_B = \int_0^{\xi_1} \frac{d\xi}{W_{SC}} . \qquad 5.1$$

However, from Fig. 6 it is seen that the integrand is infinite at $\xi = 0$. The physical explanation of this is that the starting shock wave, in moving from the nozzle throat at $\bar{A} = 1$ to the area $\bar{A} = 1 + \delta\bar{A}$, sheds a backward facing Mach wave which will remain at the nozzle throat. However, the subsequent backward facing waves generated by the further movement of the starting shock wave will all be swept through the nozzle. Hence, the numerical integration of equation 5.1 (using Fig. 6) must be performed from some position of the backward facing wave close to the nozzle throat, this position being found experimentally.

The end of the steady flow duration in the working section occurs when the contact surface, originating at the rupture of the main diaphragm, reaches the test section. The time taken, t_C , for the contact surface to move from the nozzle throat to the efflux is

$$t_C = \int_0^{\xi_1} \frac{d\xi}{u_{SC}} . \qquad 5.2$$

The graphs of u_{SC}/a_1 against $\bar{A}$ are included in Fig. 6a and 6b for equilibrium and frozen steady flows.

It is evident from the geometry of Fig. 7 that the duration of steady flow in the working section, $t_{R\,W\,S.}$, is given by the relationship

$$t_{R\,W.S.} = t_R^* + t_C - t_B . \qquad 5.3$$

Therefore, using equations 5.1 to 5.3 and equation 2.1 with Fig. 6a and 6b a pessimistic estimate of $t_{R\,W.S.}$ may be made for any particular shock tunnel geometry and initial conditions.

6. THE APPARATUS.

Details of the construction of the small 1½" square shock tube and of the associated electronic shock wave detection and triggering systems used in the experimental work described here may be found in references 12 and 13. However, briefly we note that the 1½" square channel of the shock tube was approximately 16 ft. long and the 3" I.D. driver section was 4 ft. long. Eleven instrument stations were situated in the channel and were spaced at 1½ ft. intervals. The station furthest from the main diaphragm was 4.375 ins. from the end of the channel and for the investigation into the nozzle starting process contained a barium titanate shock wave detector (see reference 12) which was used to initiate the operation of the electronic apparatus associated with the various probes placed inside the nozzle.

The vacuum in the channel was measured using two Wallace and Tiernan absolute pressure gauges, one reading 0(0.5) 100 mm.Hg., the other reading 0(2) 800 mm.Hg. Driver pressures were measured using two Budenberg standard

test gauges, one reading 0(2)400 psig., the other reading 0(50)2000 psig.

The nozzle coupled directly onto the end of the channel, the relevant dimensions being shown in Fig. 8. Details of the construction of the nozzle and plenum chamber may be found in reference 13. The nozzle was two-dimensional, three values of expansion angle being available, namely 10°, 15° and 20°. Hence, when the maximum expansion angle was used, the nozzle efflux had dimensions of ¾" by approximately 12". Three 7" D. instrument ports were available in each side plate of the nozzle and instruments could be set anywhere in the plugs situated in these ports. Normally, however, the instruments used in this investigation were placed close to the centres of each of the plugs. Plugs were also available which contained schlieren windows, giving a 6" D. viewing area at any port.

The nozzle exhausted directly into a 5 ft. long, 20" I.D. plenum chamber which was evacuated by an Edwards 9B3 vapour booster pump backed by an Edwards ISC450A rotary vacuum pump. A 9" D. pumping line connected the vacuum pumps to the plenum chamber, a large pumping line diameter being employed to make full use of the high pumping rate of the vapour booster pump at high vacuum. Care was observed in the arrangement of the vacuum seals and in the cleanliness of the internal surfaces of the nozzle and plenum chamber so that not only was the evacuation rate high but the ultimate vacuum (better than 1 micron Hg.) could be maintained for a short period prior to each experiment. Vacua were measured in the plenum chamber with an Edwards Pirani Gauge.

'Melinex' diaphragm material was used both for the main diaphragm and for the nozzle diaphragm. In the latter case, 0.00025 ins. thick Melinex was used. The use of Melinex as the main diaphragm material allowed diaphragm rupture to be obtained by using a flat nosed plunger mounted in the driver and also ensured that the driver pressures could be accurately set. However, the use of this material restricted the driver pressures to moderate levels in comparison with the higher pressures used in most reflected shock tunnels.

A cylindrical barium titanate ceramic, 6 mm. long by 2 mm. D., was used to detect the variation in stagnation pressure in the nozzle. The ceramic was surrounded in Araldite and mounted with one flat face exposed in a round-nozed probe which spanned the nozzle. Since the ceramic was sensitive to temperature changes as well as to pressure changes it was found to be necessary to cover the front face of the ceramic with, on average, four layers of Sellotape in order to reduce the temperature effects.

A stagnation point temperature probe was built and consisted of a length of glass rod which spanned the nozzle flow, a thin platinum film being baked and painted onto the rod leading edge. The rod was supported between metal jaws, the jaws being carefully shaped to give a smooth joint between glass and metal. The output from the thin film, when supplied by a constant current, could be passed through an analogue circuit (see reference 14) to produce an indication of the changes in stagnation point heat transfer rate in the nozzle flow.

A temporary schlieren system was assembled for the purposes of these experiments. The argon jet spark light source and associated electronic

triggering apparatus used with this system were built to a design by R.J. North[x].

7. THE EXPERIMENTAL INVESTIGATION INTO THE NOZZLE STARTING PROCESS

In the experimental work described in this section hydrogen was used as the driver gas and nitrogen as both the channel and plenum chamber gas. The driver, channel and plenum chamber gases were initially at room temperature and the initial pressures in the driver and channel were arranged to give a value of the primary shock Mach number at the end of the channel close to 6.0 (the tailoring value for hydrogen driving into nitrogen.) Only one channel pressure was used throughout the major part of the investigation, viz. 13 mm. Hg.

Four values of initial plenum chamber pressure were chosen for the investigation, viz. 1, 10, 100 and 1,000 microns Hg. (13,000 microns Hg. was also used with the 20° nozzle).

Only two values of nozzle angle were used, namely 10° and 20° total angle. Instruments were placed at distances of 7½ ins., 17 ins., and 26½ ins. from the nozzle diaphragm for both values.

The stagnation temperature probes and heat transfer rate analogue circuit initially produced records which showed an inacceptable level of 'noise'. This was felt to be due to bombardment of the probe by fine nozzle diaphragm particles. To eradicate this effect the probe was set approximately ¾ in. off the centre line of the nozzle and the ends of the probe near the nozzle walls were masked with Sellotape. This proved effective in reducing the 'noise' to an acceptable level.

In the experimental programme the primary shock velocity was monitored over the final 3 ft. measuring arm at the end of the channel. On average the primary shock Mach number was approximately 5.90. The trigger pulse, provided by the shock wave detector which formed the downstream end of the above velocity measuring arm, was used with a variable delay unit to trigger the sweep of the oscilloscope. Some typical oscilloscope records of the output of the stagnation temperature probe and analogue circuit are shown as examples (b), (c) and (d) on Plate I. The results obtained from these records are shown in Fig. 9 to 12 for the 10° nozzle angle and in Fig. 13 to 17 for the 20° nozzle angle. At least two records were obtained at each position and at each plenum chamber pressure. The experiments were then repeated using the stagnation pressure probe to detect the nozzle starting waves. However, it was found that at plenum chamber pressures of 10 microns Hg. and less the stagnation pressure probe responded to the arrival of the starting shock wave with a negative-going signal, instead of the usual positive signal. This effect was ascribed to the high gas temperatures behind the starting shock wave and the pyroelectric sensitivity of the barium titanate. Attempts to decrease this effect by placing more Sellotape over the exposed face of the

---

[x] Design reproduced by permission of the Director, The National Physical Laboratory.

ceramic produced encouraging results but made the effective response time of the system far too high. Specimen oscilloscope records of the output of the stagnation pressure probe, at initial plenum chamber pressures greater than 10 microns Hg., are shown in examples (e) and (f) in Plate I.

In a few of the experiments mentioned above the static pressure near the end of the channel was measured, using the barium titanate transducer set at a distance of 4.375 ins. from the end of the channel. A typical oscilloscope record of the transducer output is shown in example (a) of Plate I.

In order to investigate the effects of viscosity on the nozzle starting process, a few experiments were performed in which the initial pressures of driver, channel and plenum chamber were all increased by a factor of 2.5. As will be seen from the analyses of sections 3 to 5, in which the action of viscosity is entirely ignored, the velocities of the starting waves in the nozzle should remain virtually unchanged by this overall increase in initial pressures. The experiments were performed at these different initial pressure conditions using the stagnation temperature probe which was set at the furthest position from the nozzle diaphragm so as to reduce the pressure loads on the glass probe. Conditions were investigated at only two values of initial plenum chamber pressure, namely 2,500 microns Hg. and 25 microns Hg. The results of these experiments are included in Fig.14 and 16 for comparison.

Some experiments were performed using the 20° nozzle angle and the schlieren system mentioned in section 6. The photographic results were not very good, due to the insensitivity of the optical system and it was possible to detect the starting shock wave only at the highest values of plenum chamber pressure used.

8. COMPARISON OF THEORY AND EXPERIMENT FOR THE NOZZLE STARTING PROCESS.

The experimental results are shown in Fig. 9 to 12 for the 10° nozzle angle and in Fig. 13 to 17 for the 20° nozzle angle. Included in all the figures are the theoretical curves for the starting wave trajectories obtained from the analyses of sections 3 to 5.

The trajectories of the forward starting shock wave shown in the above figures have been calculated from the numerical integration of equation 3.3. It is seen that, at all the conditions considered and summarised in Fig. 9 to 17, the trajectories for the forward facing shock wave obtained from the analysis of section 3 are in close agreement with the experimental data. When the allowances for real gas effects on the initial strength of the forward facing shock wave (see section 3) are made, it is seen that, in general, an improvement in the correlation between theory and experiment results.

The trajectories of the backward facing waves shown in Fig. 9 to 17 have been calculated from the numerical integration of equation 5.1, using the wave velocity curves of Fig. 6. In order to avoid the singularity occurring at the throat (mentioned in section 5) the method of calculation adopted was to assume a mean value of wave velocity between the area ratios of one and two. Both the frozen and equilibrium 'steady' state calculations of section 4 are included.

In general, the calculations based on equilibrium steady flow show a closer correlation with the experimental data than do the calculations based on frozen steady flow. However, Stollery and Townsend[11] have shown that the steady flow may be frozen. It was suggested in section 4 that the trajectories of the backward facing waves obtained by experiment should always lie below the trajectories of the 'steady' state calculations of section 4. Consequently, the fact that the actual trajectories of the backward facing waves agree quite closely with the equilibrium steady flow calculations may be coincidental.

The data from the experiments in which the initial pressures in driver, channel and plenum chamber were increased by a factor of 2.5 compare quite well with the more extensive data obtained at the lower pressures. However, whilst the experimental results for the cases where the plenum chamber pressures were 2,500 microns Hg. and 1,000 microns Hg. are in good agreement, the same cannot be said for those at 25 and 10 microns Hg. It is seen in Fig. 14 that when p_N = 25 microns Hg., the starting shock wave appears to travel through the nozzle at a slightly higher velocity than in the case where p_N = 10 microns Hg. and at a higher velocity than that predicted by Chisnell's analysis. Assuming that the action of viscosity is such as to increase the starting shock wave attenuation as the pressure decreases then the inference is that the application of Chisnell's analysis to the present problem results in an underestimate being made of the starting shock wave velocity. This apparent error may be due to the presence of the contact surface in the present problem which does not occur in Chisnell's model. Calculations reveal that if backward facing compression waves are shed by the starting shock wave in its interaction with the nozzle walls then in the cases of p_N = 10 and 25 microns Hg. the reflections of these waves at the contact surface would be such as to increase the strength of the starting shock wave. However, in the cases of p_N = 1,000 and 2,5000 microns Hg. the reflections of the backward facing waves would be so weak as to hardly affect the strength of the starting shock wave.

It is to be noted that some of the records of stagnation point heat transfer rate and stagnation pressure show a steady increase in these two quantities once the starting waves have passed the observation point (see example (c) on Plate I). This may be due to the growth of the boundary layers on the nozzle walls. It is difficult to establish how this will affect the nozzle starting process. However, it seems likely that should viscosity affect significantly the various strengths of starting waves examined in the present experimental investigation, the effects should vary widely over the range of starting wave strengths examined. Since this does not appear to be the case it seems likely that the action of viscosity in the steadily expanding flow has little effect on the nozzle starting process.

With regard to the steadiness of the expanding gas through the nozzle, it must be remembered that the reservoir gas behind the reflected primary shock wave must also be steady. However, the experiments in which the static pressure was measured close to the end of the channel show that this is not the case. When the reflected shock wave has passed the transducer it is seen that the pressure continues to rise but then falls again. The continuing rise in pressure after the passage of the reflected shock wave has been attributed to the interaction between the reflected shock wave and the boundary layer created by the primary shock wave (see reference 5). However, the subsequent

fall in pressure, shown in example (a) of Plate I, remains inexplicable. It is noted that, as shown in example (a) of Plate I, the reflected head of the rarefaction wave (RR) curtails the flow of the hot test gas in this particular shock tunnel.

9. CONCLUDING REMARKS.

In the discussion of sections 2 to 5 of the running times to be expected in the working sections of hypersonic reflected shock tunnels, it has been shown that an estimate must first be made of the duration of steady, high enthalpy gas flow at the nozzle throat. The remainder of the discussion is then concerned with explaining the differences between the steady flow duration at the nozzle throat and at the hypersonic working section in the light of the strength and nature of the nozzle starting process. In comparing, in section 8, the analyses of sections 3 to 5 with the experimental results obtained in the present investigation it is shown that the trajectories of the starting waves can be quite adequately predicted for values of efflux to throat area ratios lower than 100. Consequently, it is suggested that further experimental data are required for area ratios up to, say, 10^4, this order of magnitude being common for reflected shock tunnels. In performing these experiments, it may be worthwhile to examine the effects of viscosity on the nozzle starting process by investigations carried out at various different overall pressure levels, whilst maintaining the primary and nozzle diaphragm pressure ratios approximately constant.

No analysis has yet been produced which describes the continuous growth of the backward facing wave in the nozzle and this problem calls for further investigation.

In order to obtain the maximum possible steady flow duration in the working section it is necessary to increase the nozzle diaphragm pressure ratio for increasing values of efflux-to-throat area ratio. Assuming that it is preferable to maintain the advantages of the tailoring condition and that there is a limit to the driver pressure it is therefore necessary to ensure that the plenum chamber and nozzle may be evacuated initially to the order of 1 micron Hg. pressure.

ACKNOWLEDGEMENTS.

Thanks are due to Dr. L.G. Whitehead for his help and interest in the design and construction of the apparatus used in the present experimental investigation. To Dr. L. Bernstein the author wishes to make known his gratitude for the many useful discussions concerning practical and theoretical matters. Thanks are also due to Mr. W.H. Montague who built much of the apparatus, particularly in the construction of the vacuum systems. Finally, the author would like to thank Professor A.D. Young for his interest, encouragement and many helpful comments in the preparation of this paper.

10. NOTATION.

a_i	speed of sound in region i.
A_{ij}	speed of sound ratio a_i/a_j.
A'	area
K	index of variable value defined by equation 3.1.
M	Mach number.
p_i	pressure in region i.
P_{ij}	pressure ratio p_i/p_j.
t	time.
T_i	temperature in region i.
T_{ij}	temperature ratio T_i/T_j.
u_i	velocity in region i.
U_{ij}	velocity ratio u_i/a_j.
W_i	wave speed into region i.
α_i	$= (\gamma_i+1)/(\gamma_i-1)$.
γ_i	specific heat ratio in region i.
ξ	distance from nozzle throat.
ρ_i	density in region i.

Suffices

1	refers to quantities in region ahead of primary moving shock wave.
2	refers to quantities in region immediately behind primary moving shock wave.
3	refers to quantities in region between primary contact surface and rarefaction wave.
5	refers to quantities in region behind reflected primary shock wave.
B	refers to backward facing wave in nozzle.
c	refers to conditions at the contact surface.

D	refers to conditions in the channel.
N	refers to quantities in nozzle ahead of the starting waves.
W.S.	refers to conditions in the working section.
S	refers to starting shock wave in nozzle.
S_i	refers to shock wave moving into region i.
R	refers to flow durations.
TH.	refers to quantities evaluated from simple shock tube theory.

The superscript * refers to quantities evaluated at the nozzle throat. Note that primes and bars, used with areas, refer to special areas defined individually.

11. REFERENCES.

1. J.A.D. Ackroyd — A Study on the Running Times in Shock Tubes. A.R.C. C.P. 722. July, 1963.

2. B.D. Henshall and G.E. Gadd — Factors Affecting the Performance of the Nozzle of a Hypersonic Shock Tube. A.R.C. C.P. 293. Feb. 1956

3. R.F. Chisnell — The Motion of a Shock Wave in a Channel, with Applications to Cylindrical and Spherical Shock Waves. J. Fluid Mech. 2. 286 (1957).

4. A. Hertzberg, W.E. Smith, H.S. Glick and W. Squire — Modifications of the Shock Tube for the Generation of Hypersonic Flow. Cornell Aero. Lab. Inc. Rep. No. AD-789-A-2. March 1955.

5. D.W. Holder and D.L. Schultz — On the Flow in a Reflected Shock Tunnel. A.R.C. R. and M. 3265. August 1960.

6. L. Bernstein — Tabulated Solutions of the Equilibrium Gas Properties behind the Incident and Reflected Normal Shock-Wave in a Shock Tube. A.R.C. C.P. 626. April, 1961.

7. J. Lukasiewicz — Shock Tube Theory and Applications Division of Mechanical Eng., N.A.E. Canada. Report 15. 1952.

8. R.A. Alpher and D.R. White — Flow in Shock Tubes with Area Change at the Diaphragm Section. J. Fluid Mech. 3 457 (1958).

9. W. Chester. — The Propagation of Shock Waves along Ducts of Varying Cross-Section. Advances in Appl. Mechanics VI 120, 1960.

10.	L. Bernstein	Equilibrium Real-Gas Performance Charts for a Hypersonic Shock Tube Wind-Tunnel Employing Nitrogen. A.R.C. C.P. 633. September, 1961.
11.	J.L. Stollery and J.E.G. Townsend	Pressure, Heat-Transfer and Temperature Measurements in the Two-Dimensional Nozzle of a Reflected Shock Tunnel. A.R.C. C.P. 726. September, 1962.
12.	L. Bernstein	Ph.D. Thesis. University of London. Jan. 1961.
13.	J.A.D. Ackroyd	Ph.D. Thesis. University of London. Jan. 1964.
14.	R.F. Meyer	A Heat Flux Meter for use with Thin Film Surface Thermometers. N.R.C. Canada..Rep. No. LR 279. April 1960.
15.	C.E. Smith, Jr.	An Analytic Study of the Starting Process in a Hypersonic Nozzle. Proc. Heat Transfer and Fluid Mech. Inst. Stanford Univ. Press, 1964. p.198.
16	C.E. Smith, Jr.	The Starting Process in a Hypersonic Nozzle. Univ. of Oxford Dept. of Eng. Science Rep. 1000. July, 1965.

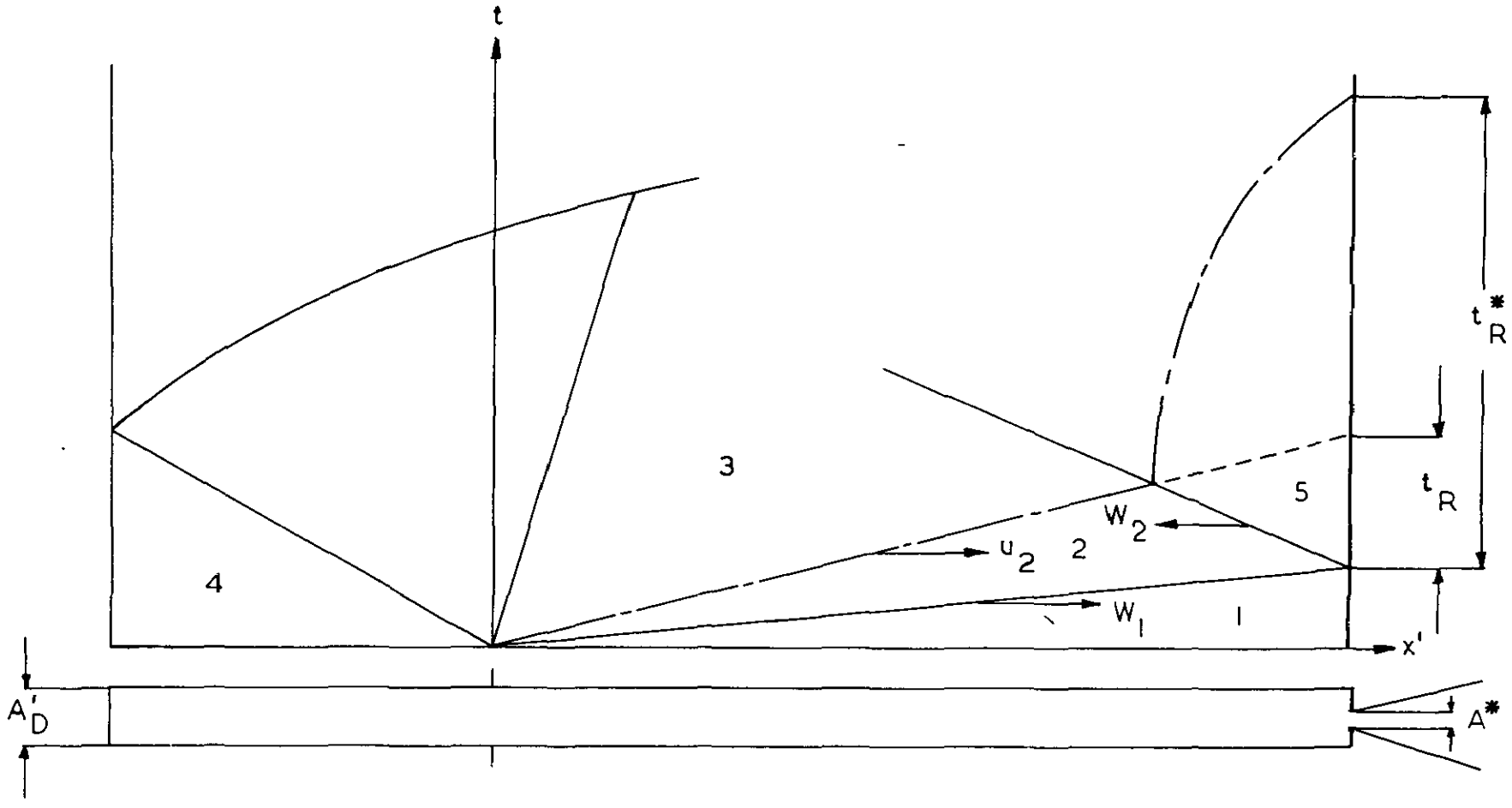

FIG 1. THE DURATION OF STEADY FLOW, t_R^*, AT THE NOZZLE THROAT OF THE REFLECTED SHOCK TUNNEL AT TAILORING CONDITIONS

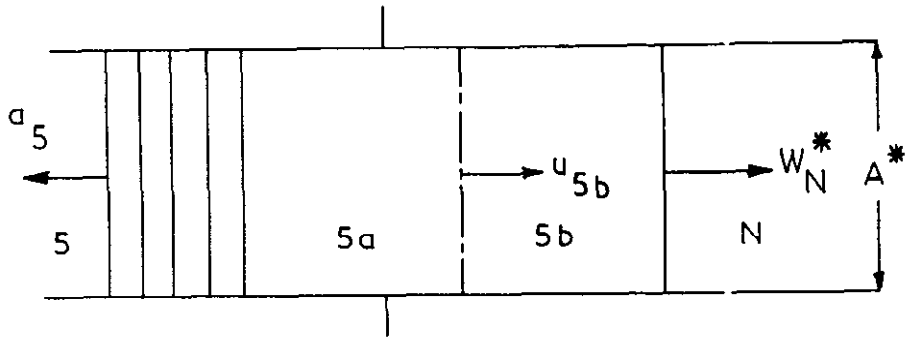

a) THE SIMPLE SHOCK TUBE MODEL WITH HEATED DRIVER GAS

b) THE SIMPLE SHOCK TUBE MODEL WITH AREA CHANGE AT POSITION OF DIAPHRAGM AND HEATED DRIVER GAS

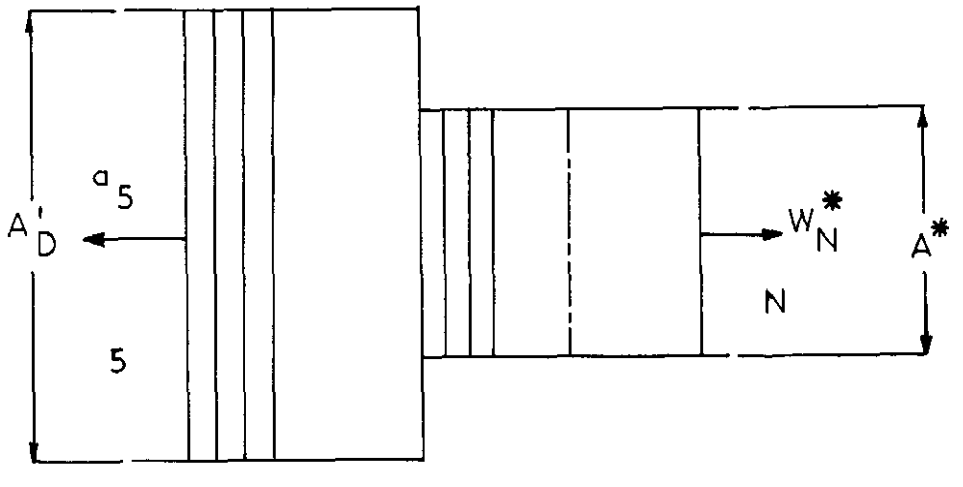

FIG 2. THE FORMULATION OF A MODEL FOR THE CALCULATION OF M_{SN}^*

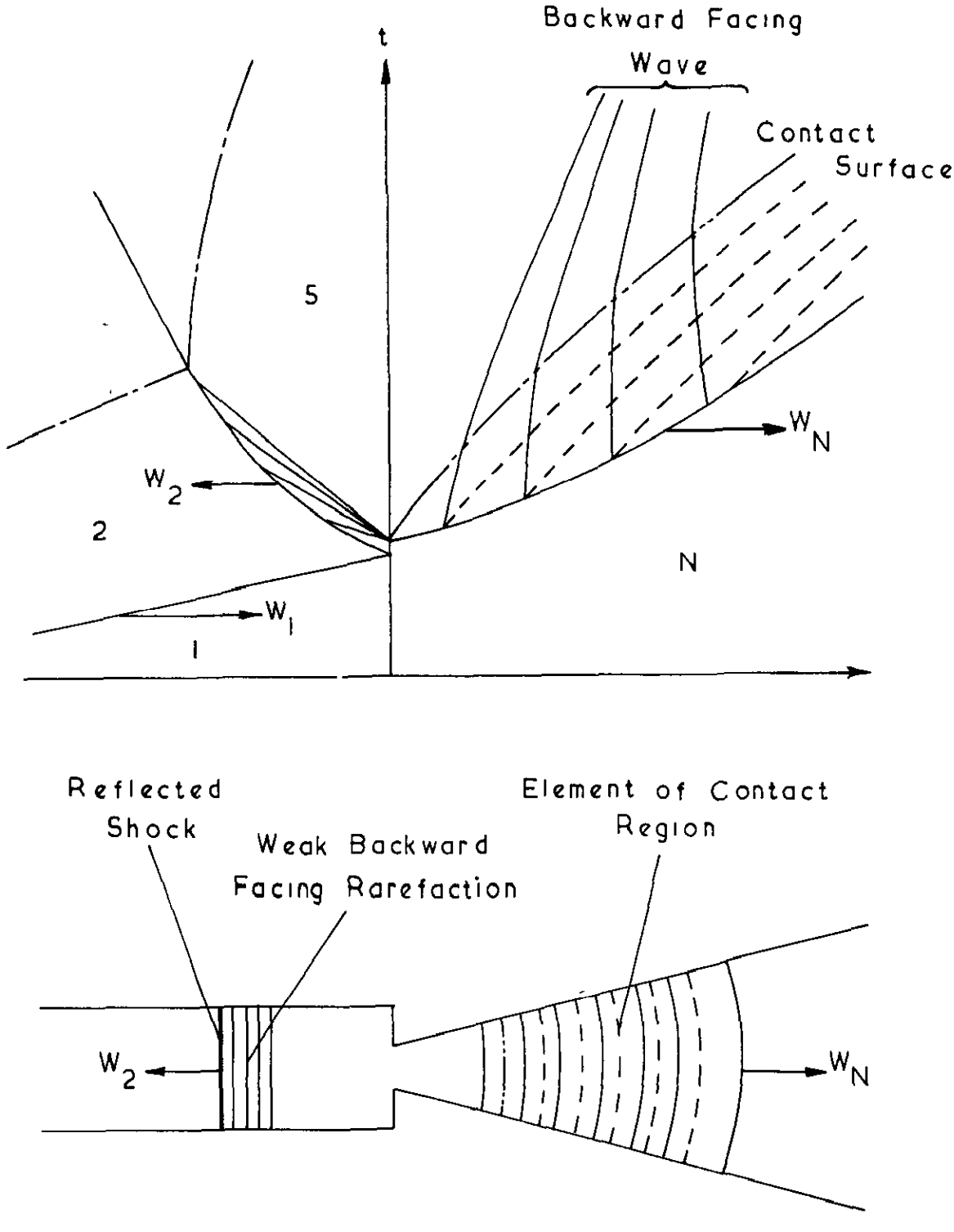

FIG 2c THE MODEL FOR THE NOZZLE

STARTING PROCESS

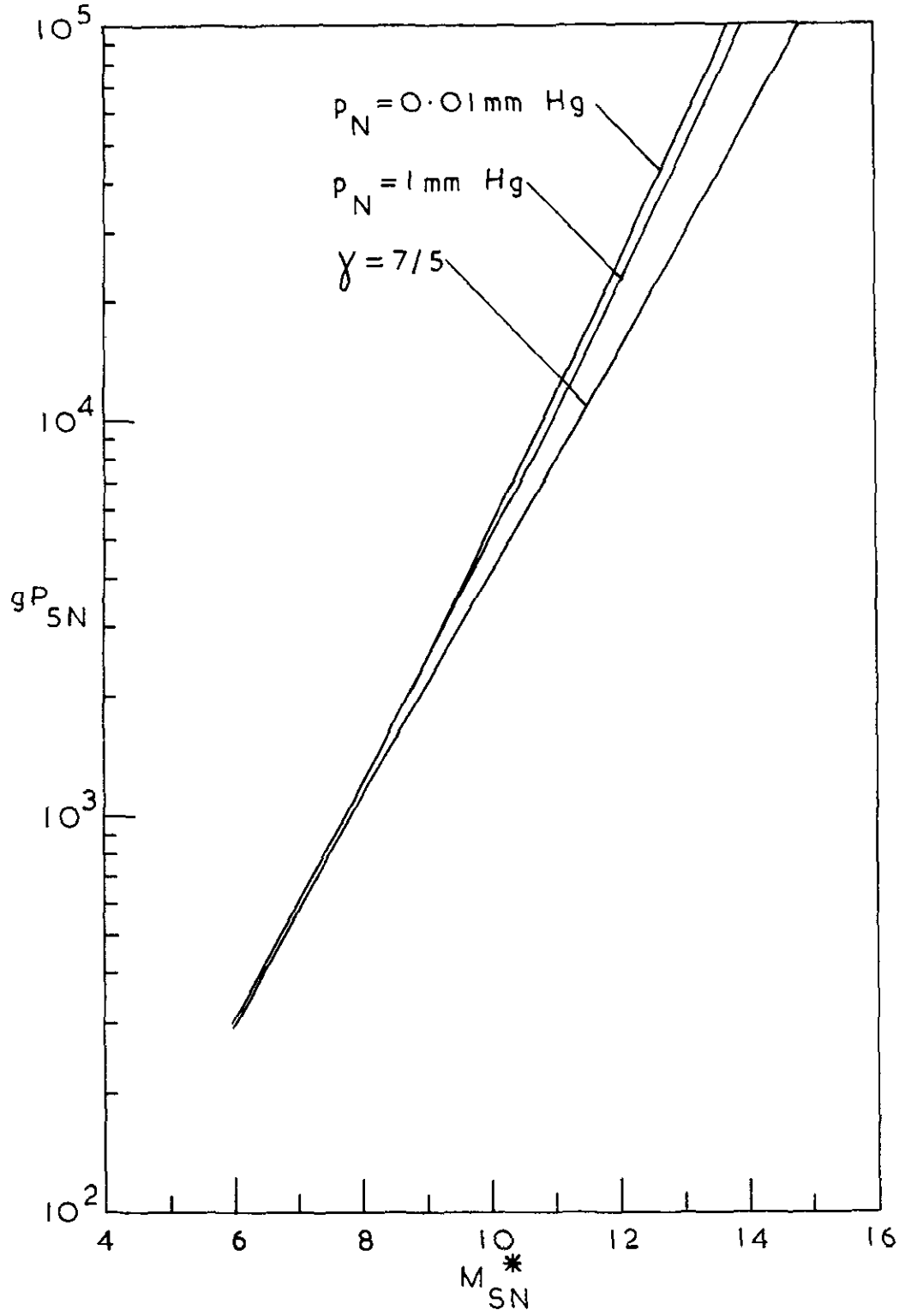

FIG 3a GRAPHS OF NOZZLE DIAPHRAGM PRESSURE RATIO, gP_{SN}, AGAINST INITIAL SHOCK MACH NUMBER, M^*_{SN} $(6 < M^*_{SN} < 16)$

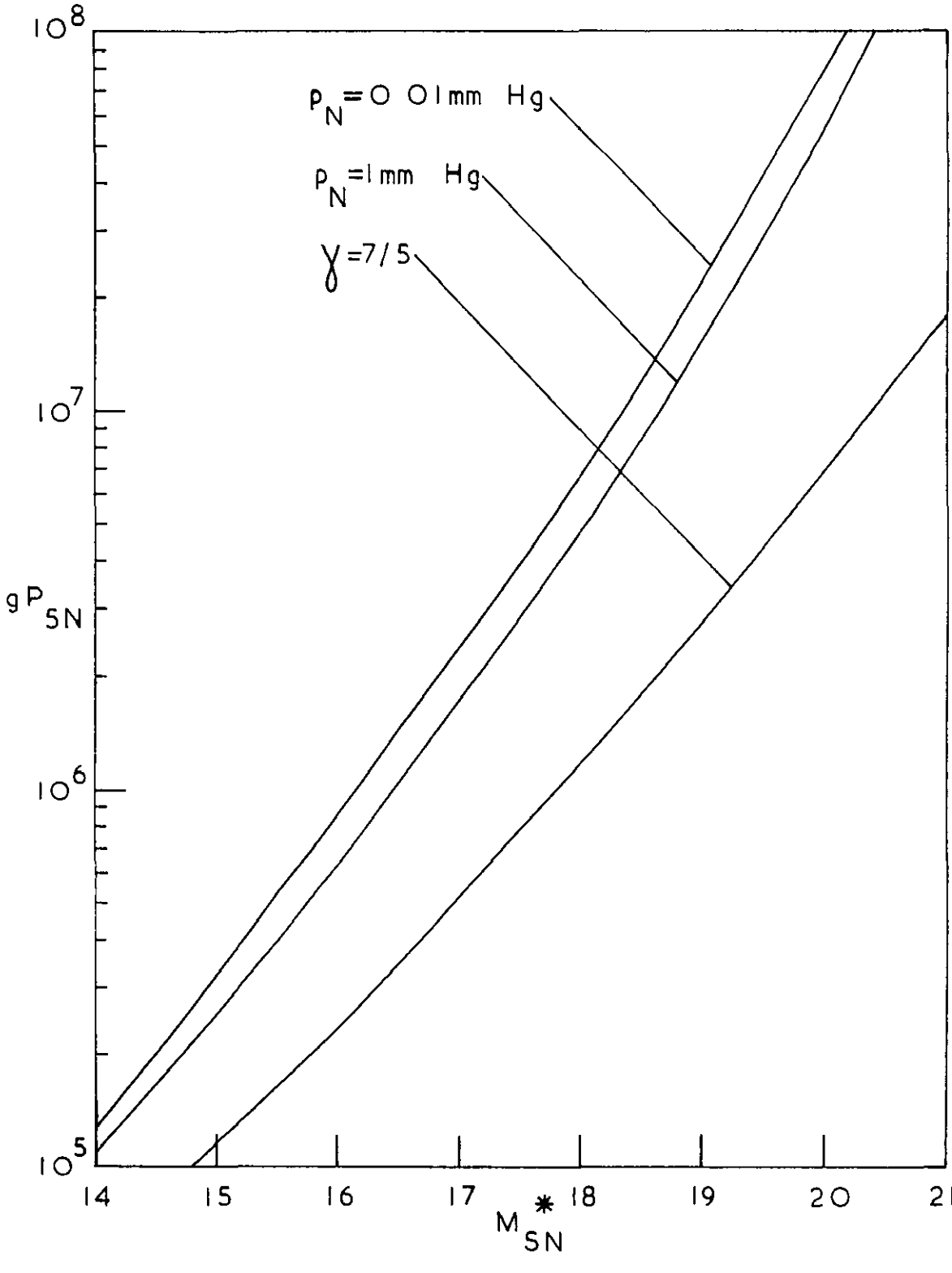

FIG 3b GRAPHS OF NOZZLE DIAPHRAGM PRESSURE RATIO, gP_{SN}, AGAINST INITIAL SHOCK MACH NUMBER, M^*_{SN}. $(14 < M^*_{SN} < 21)$

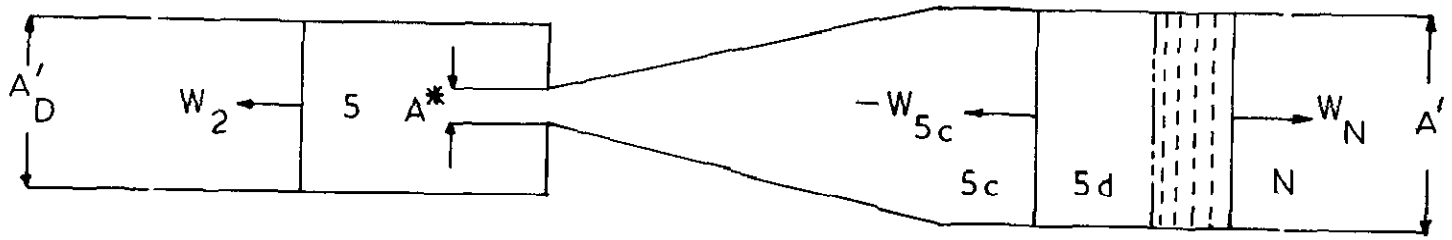

FIG 4. THE STEADY MODEL FOR THE NOZZLE STARTING WAVES.

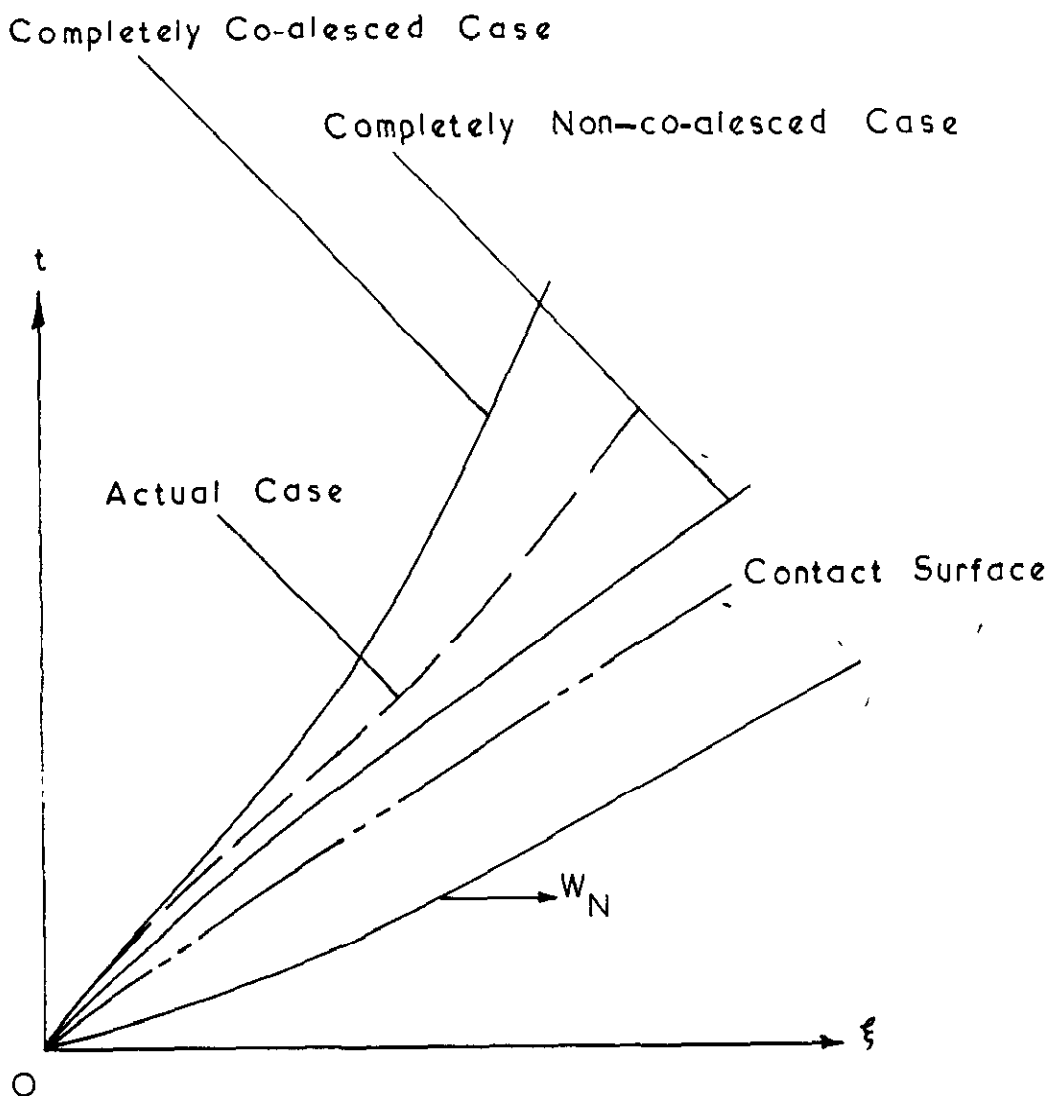

FIG 5. THE LIMITS TO THE BACKWARD FACING WAVE TRAJECTORY

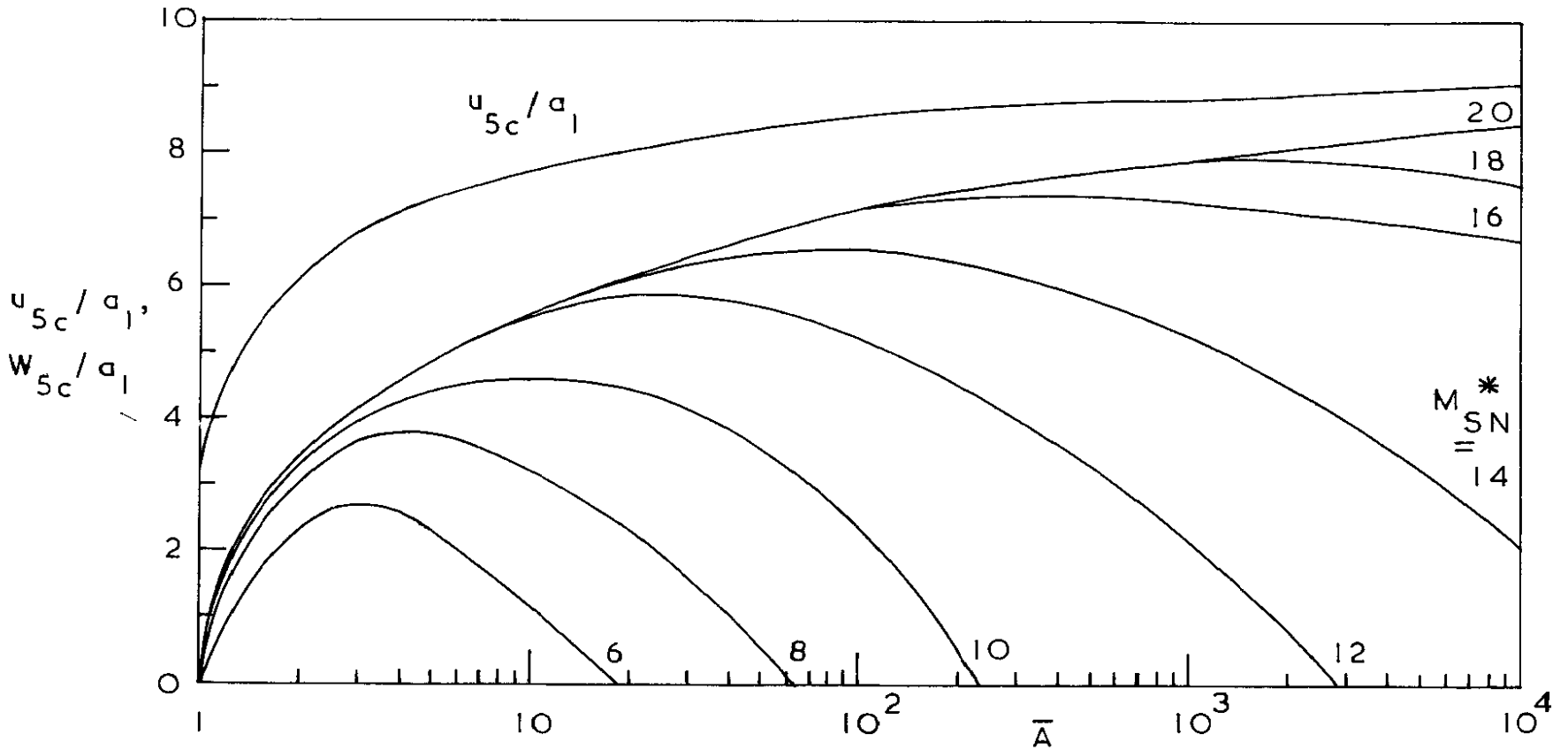

FIG 6a GRAPHS OF BACKWARD FACING WAVE VELOCITY, W_{5c}, AND GAS VELOCITY, u_{5c}, AGAINST NOZZLE AREA RATIO, $\bar{A}$ (EQUILIBRIUM FLOW)

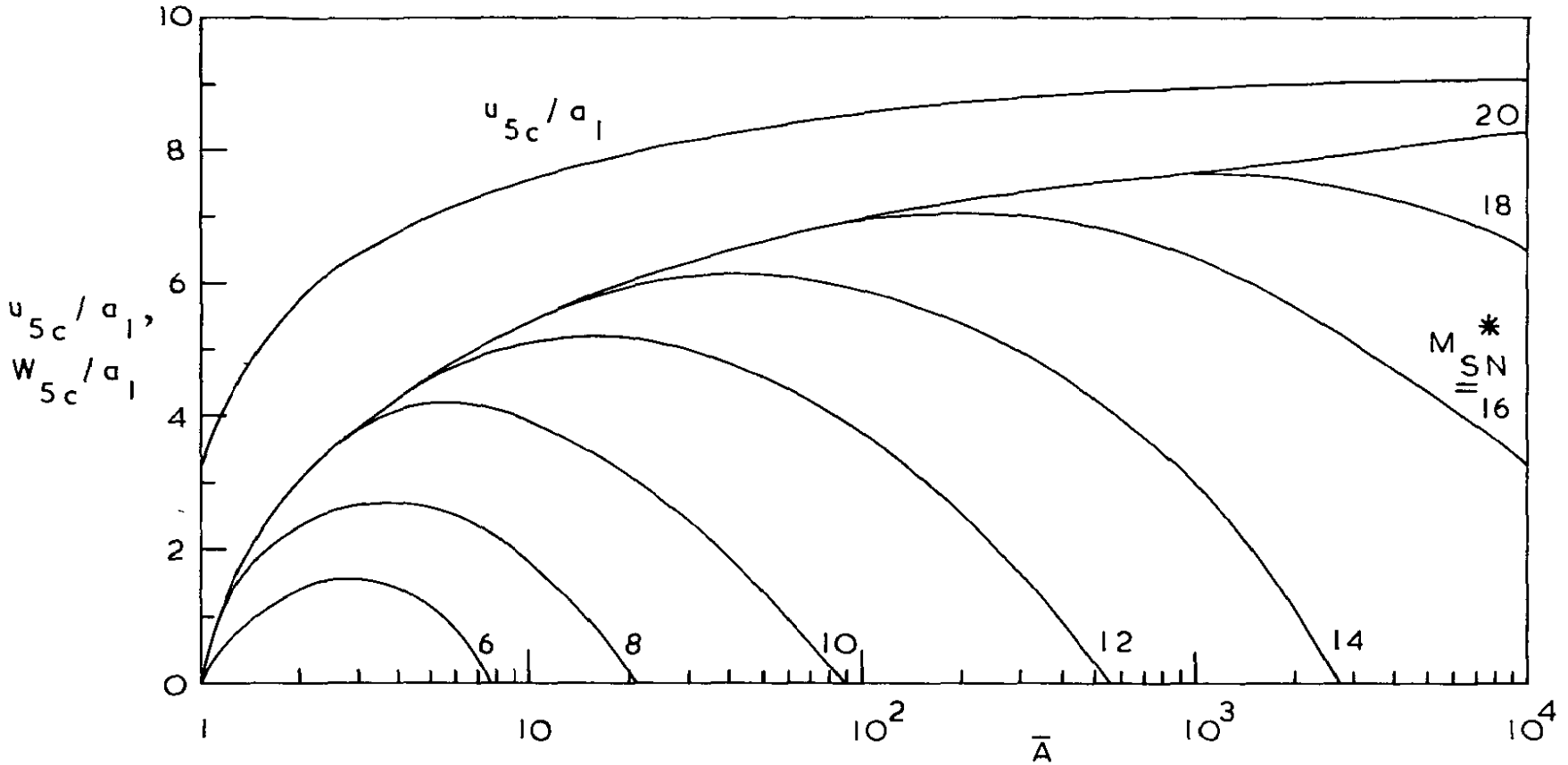

FIG 6b GRAPHS OF BACKWARD FACING WAVE VELOCITY, W_{5c}, AND GAS VELOCITY, u_{5c}, AGAINST NOZZLE AREA RATIO, $\bar{A}$ (FROZEN FLOW)

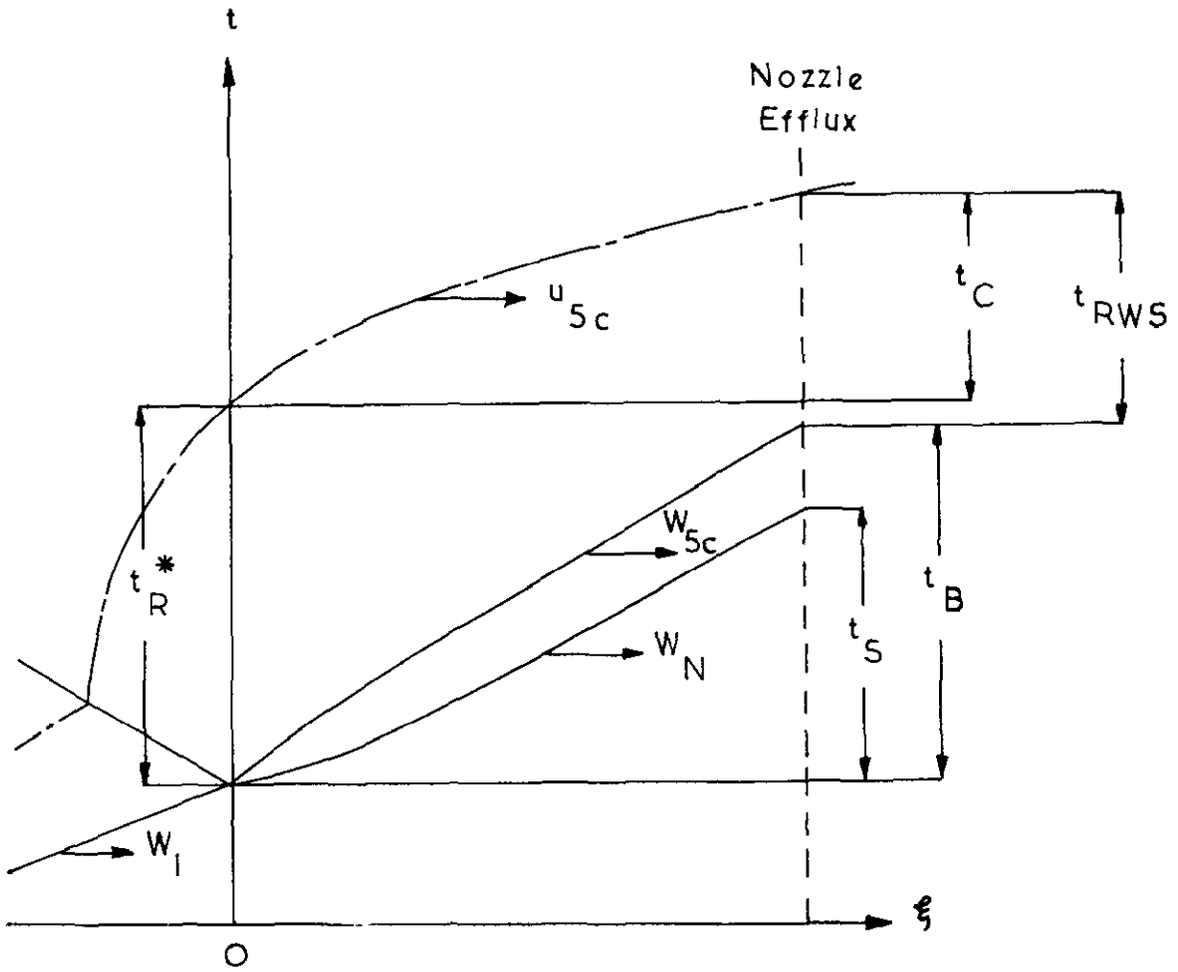

FIG 7 THE STEADY FLOW DURATION, t_{RWS}, IN THE HYPERSONIC WORKING SECTION

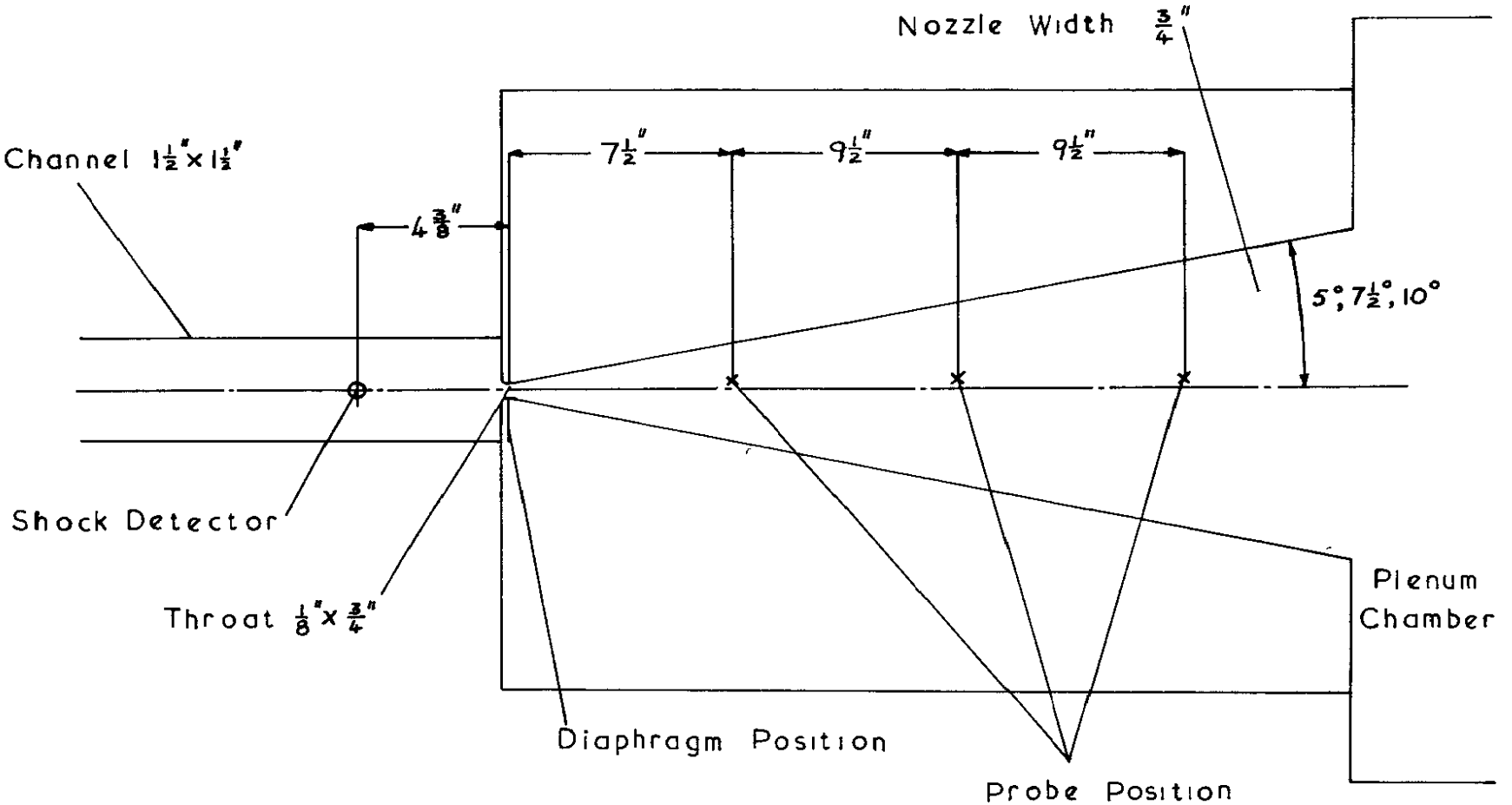

FIG 8 SKETCH OF NOZZLE

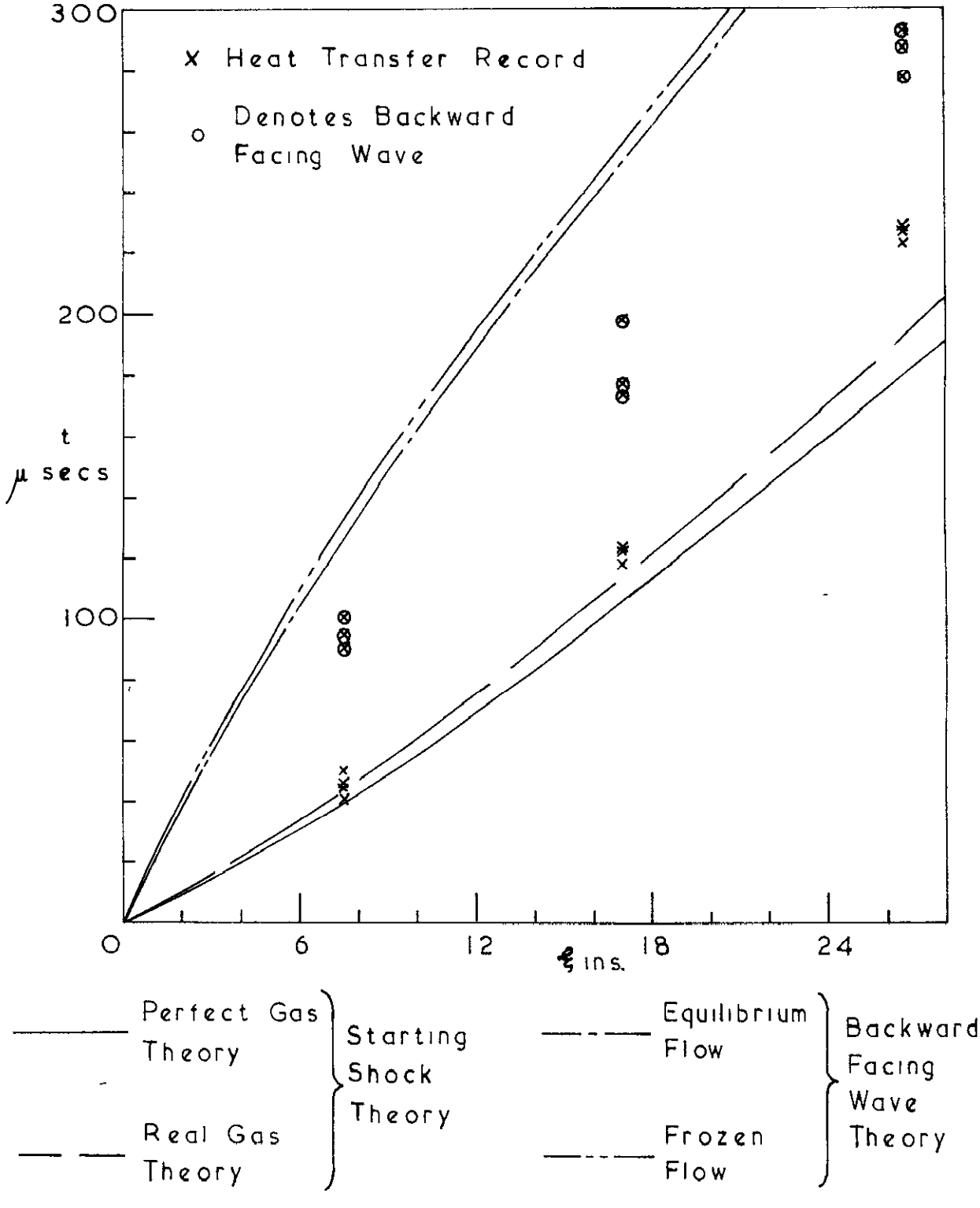

FIG 9 NOZZLE STARTING WAVES, 10° NOZZLE ANGLE, p_N=1micron Hg

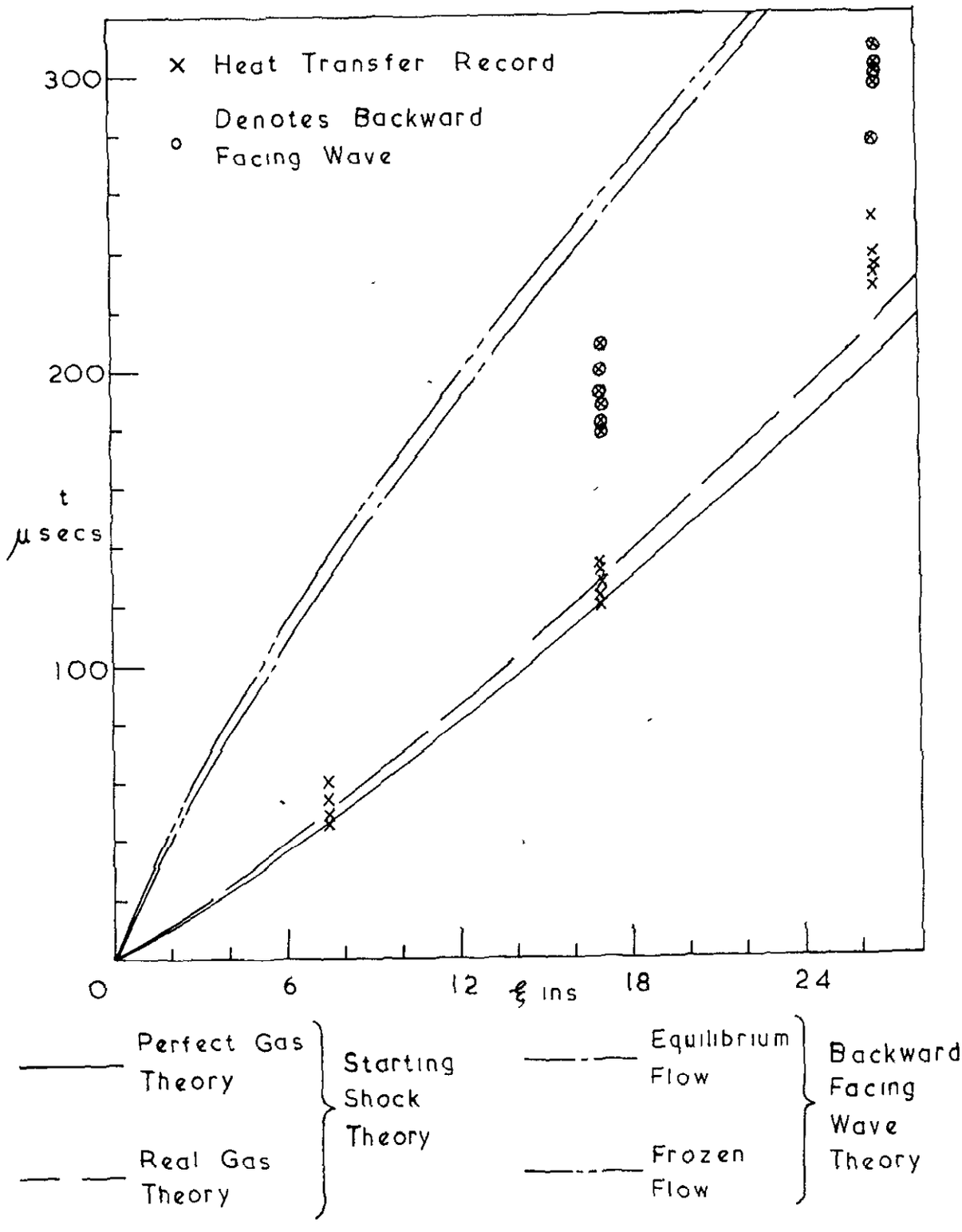

FIG 10 NOZZLE STARTING WAVES, 10° NOZZLE ANGLE, p_N = 10 microns Hg

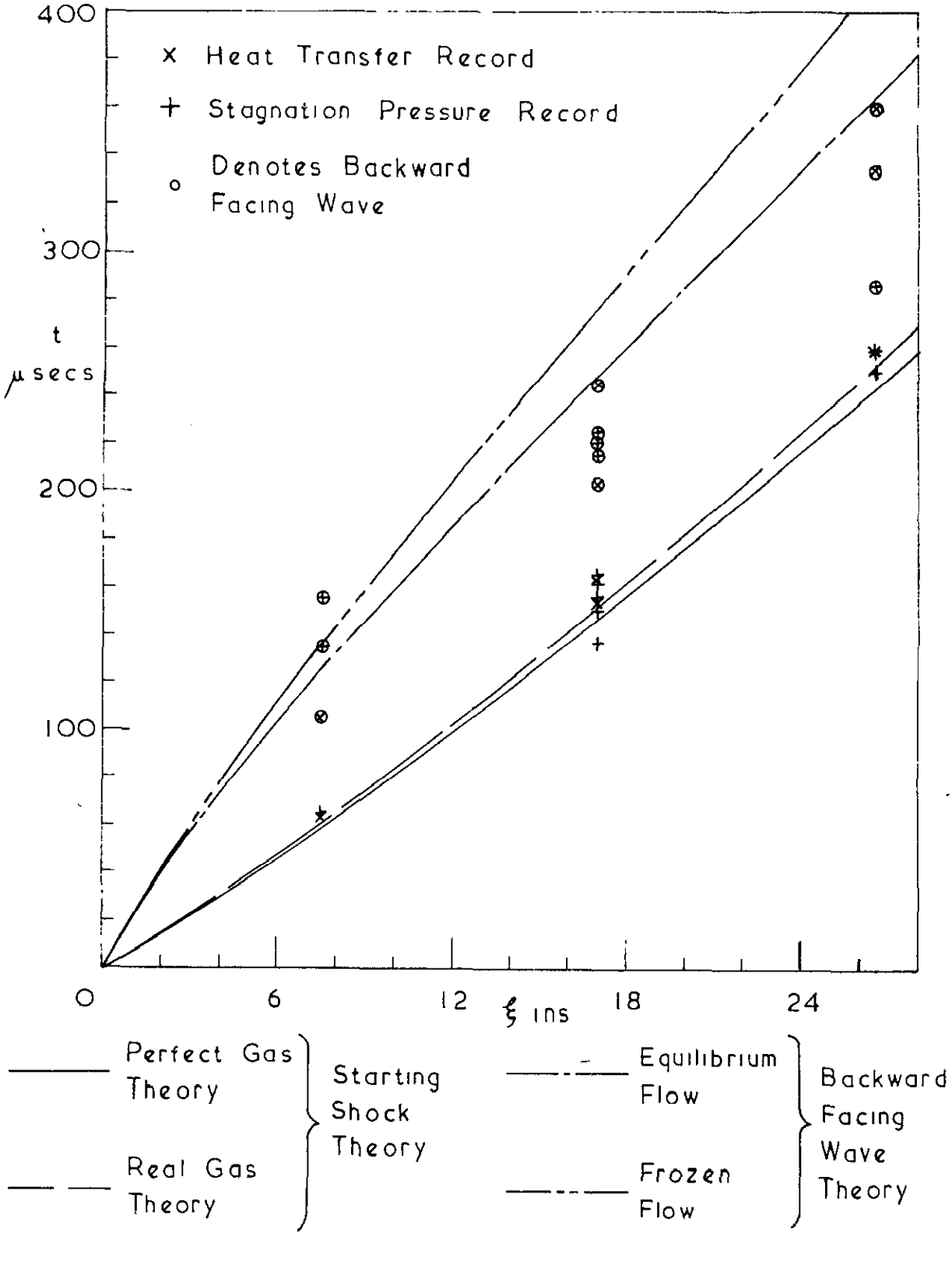

FIG 11 NOZZLE STARTING WAVES, 10° NOZZLE ANGLE, p_N = 100 microns Hg

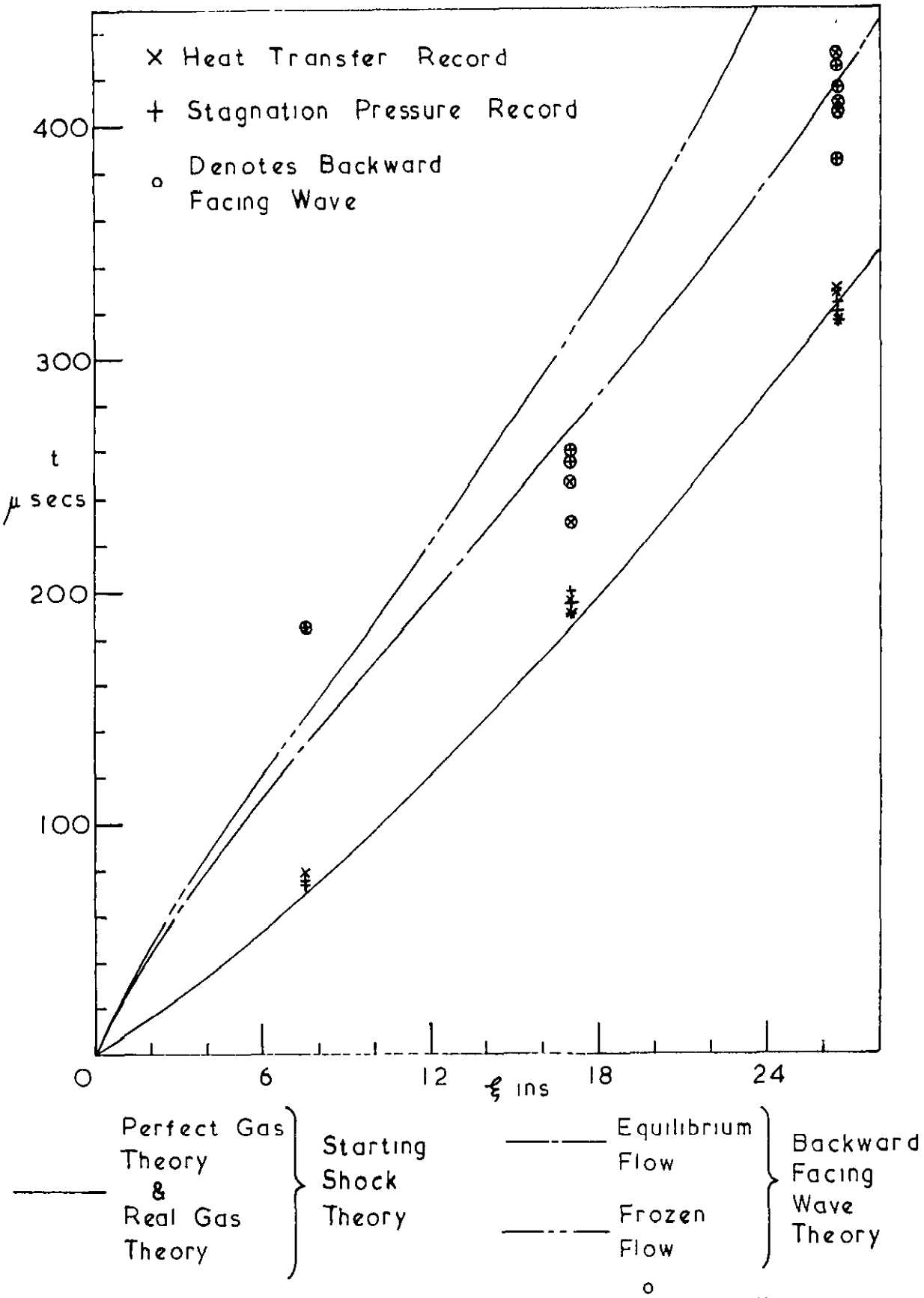

FIG 12. NOZZLE STARTING WAVES, 10° NOZZLE ANGLE, $p_N = 1000$ microns Hg

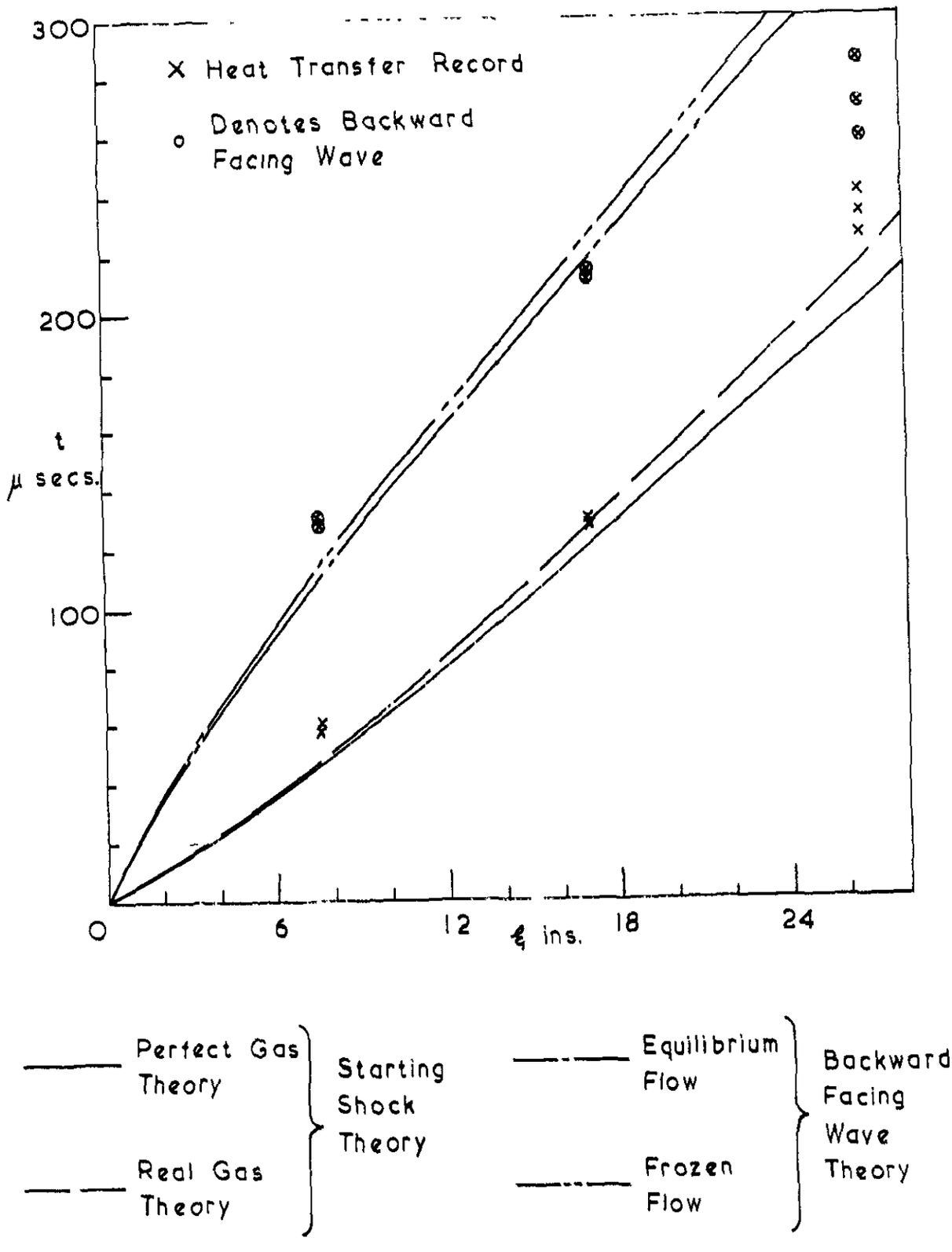

FIG. 13 NOZZLE STARTING WAVES, 20° NOZZLE ANGLE, p_N = 1 micron Hg.

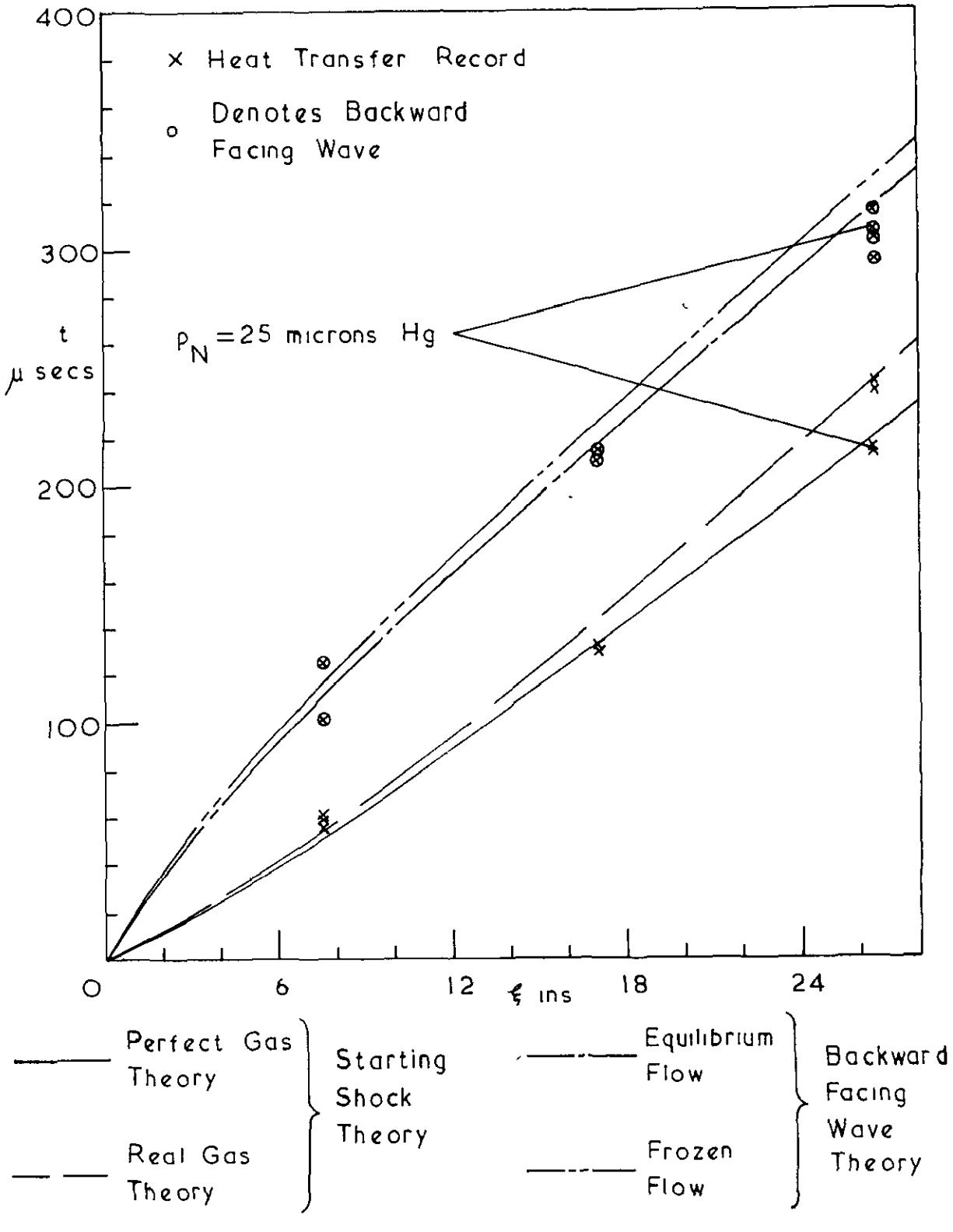

FIG 14. NOZZLE STARTING WAVES, 20° NOZZLE ANGLE, p_N = 10 microns Hg

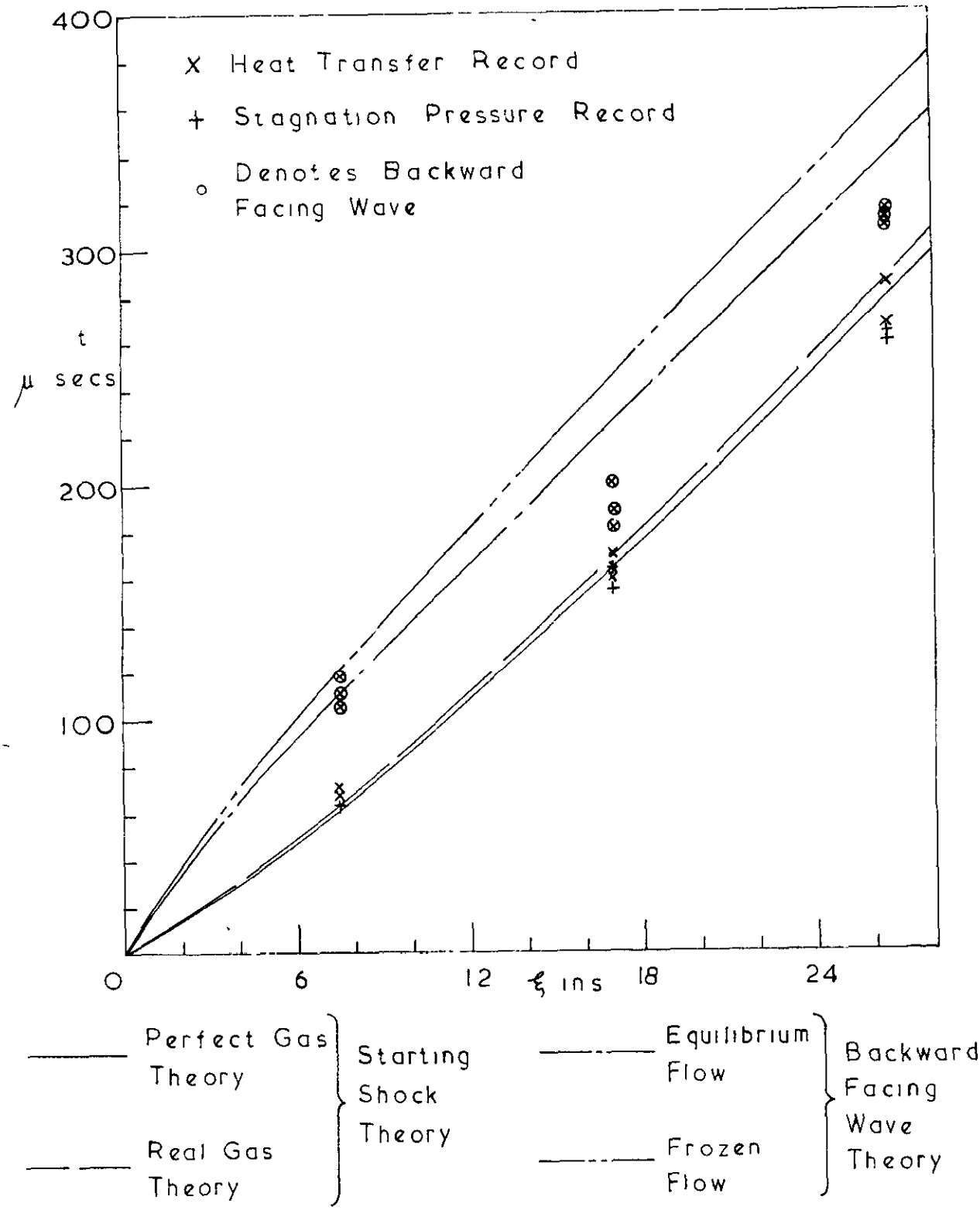

FIG 15. NOZZLE STARTING WAVES, 20° NOZZLE ANGLE, p_N = 100 microns Hg

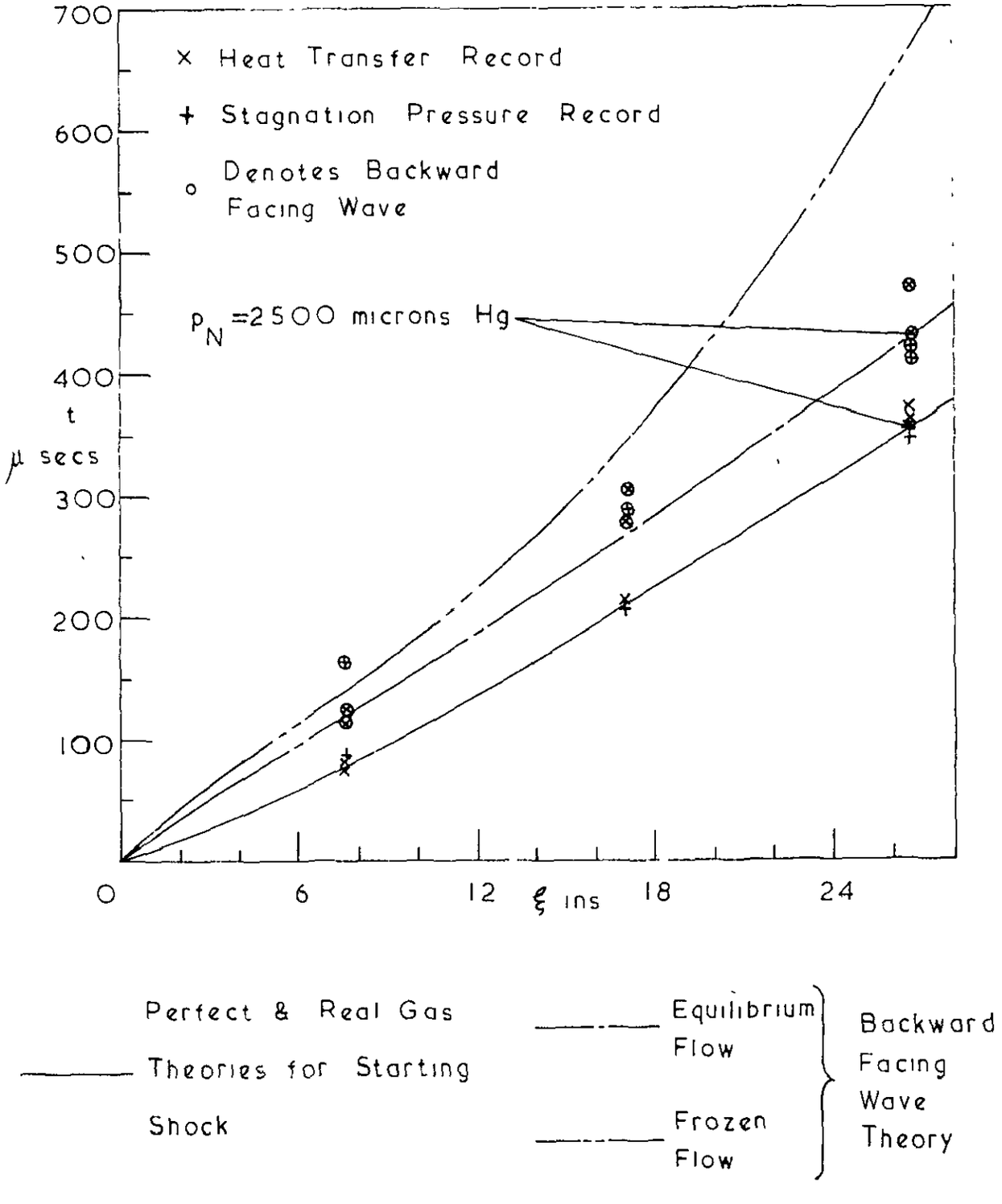

FIG 16 NOZZLE STARTING WAVES 20 NOZZLE ANGLE p_N = 1000 microns Hg

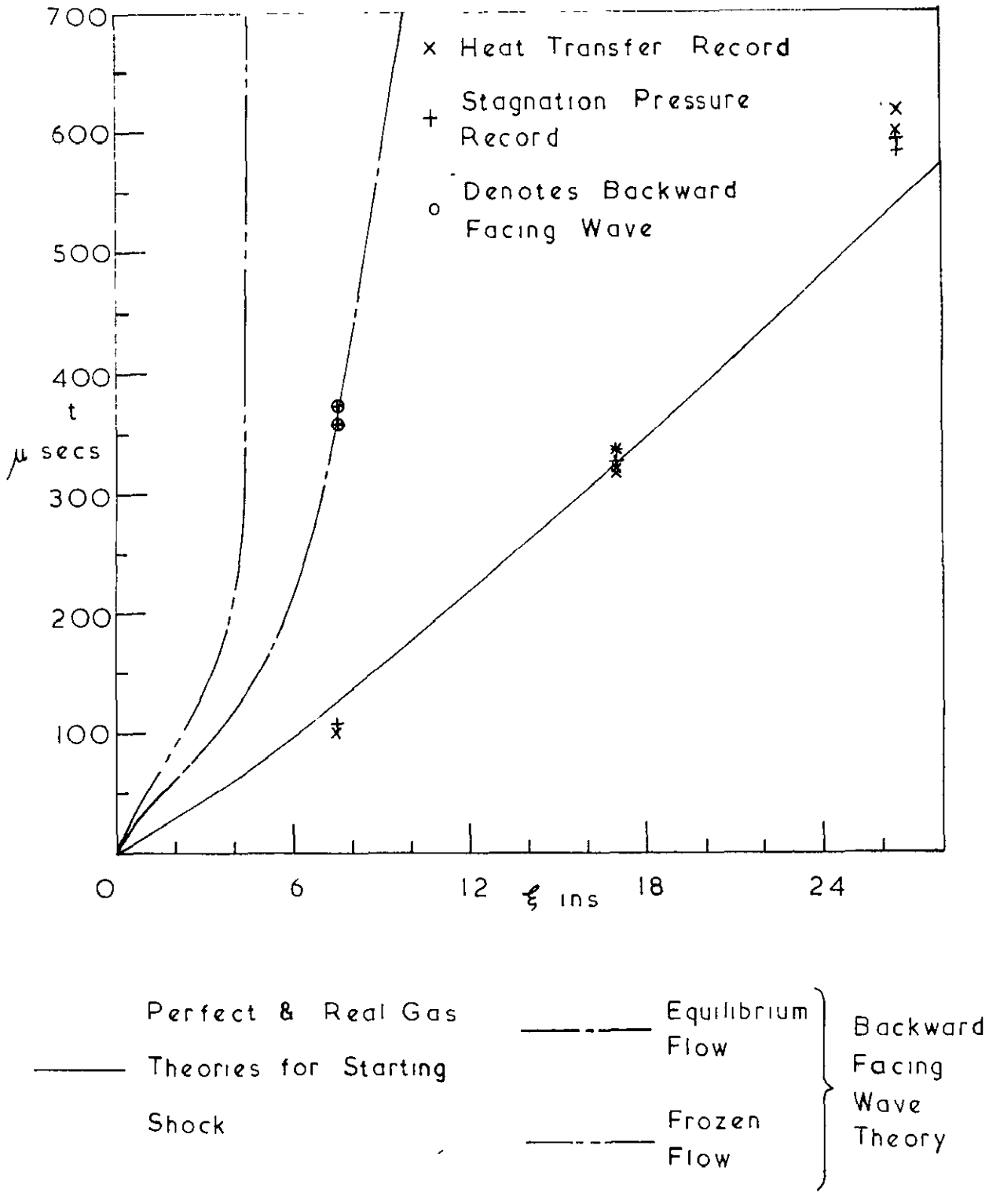

FIG 17. NOZZLE STARTING WAVES, 20° NOZZLE ANGLE, p_N = 13000 microns Hg

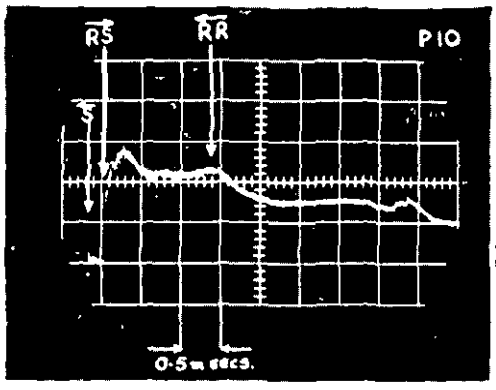

(a)

Static pressure in channel, $x' = 15{\cdot}896$ ft,
$p_1 = 14{\cdot}0$ mm Hg, Local $M_{S_1} = 6{\cdot}04$

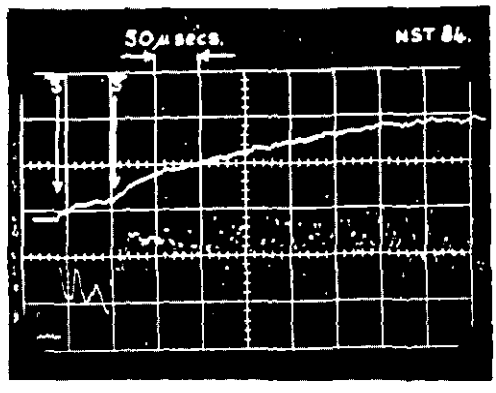

(b)

Stagnation temperature probe in nozzle
10° Nozzle Angle, $\xi = 26{\cdot}5$ in., $p_N = 1000$ microns Hg

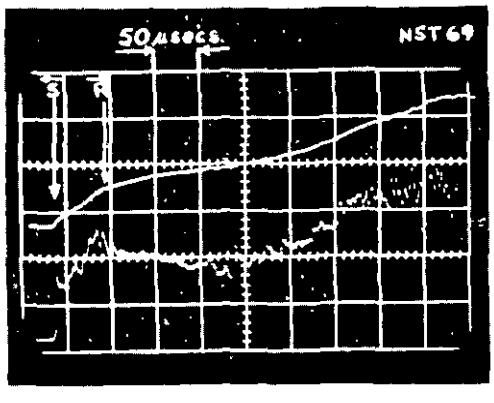

(c)

Stagnation temperature probe in nozzle.
10° Nozzle Angle, $\xi = 17{\cdot}0$ in., $p_N = 10$ microns Hg

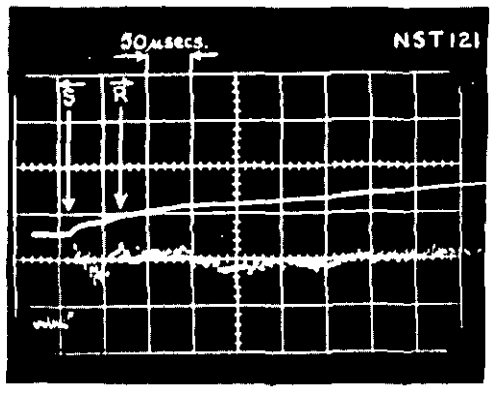

(d)

Stagnation temperature probe in nozzle.
20° Nozzle Angle, $\xi = 7{\cdot}5$ in., $p_N = 1$ micron Hg

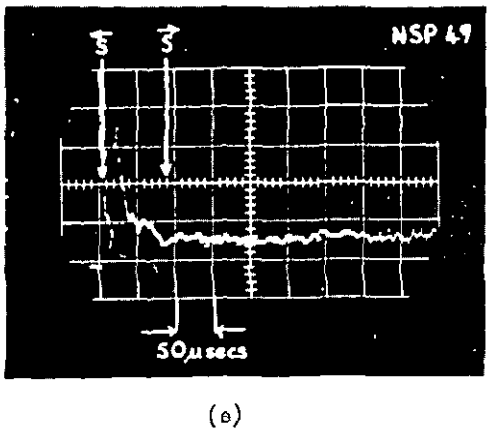

(e)

Stagnation pressure probe in nozzle.
20° Nozzle Angle, $\xi = 17{\cdot}0$ in., $p_N = 1000$ microns Hg

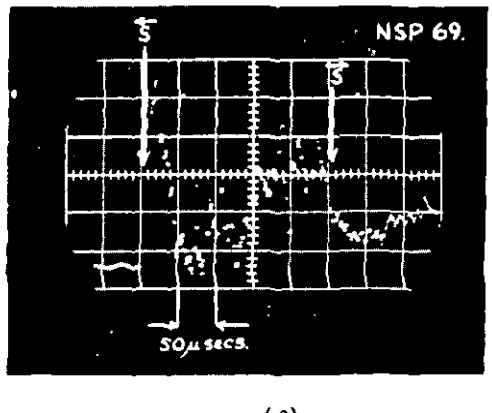

(f)

Stagnation pressure probe in nozzle
20° Nozzle Angle, $\xi = 7{\cdot}5$ in., $p_N = 13\,000$ microns Hg

PLATE I. SPECIMEN RECORDS OBTAINED IN THE NOZZLE

A.R.C. C.P. No. 883
January, 1965
Ackroyd, J. A. D.

A STUDY ON THE RUNNING TIMES IN REFLECTED SHOCK TUNNELS

The running time obtainable in a reflected shock tunnel is considered, particular attention being paid to the nature of the unsteady wave starting process in the nozzle. A range of initial conditions has been examined experimentally in a two-dimensional nozzle with a maximum efflux-to-throat area ratio of 100. An approximate analysis based on Chisnell's theory is shown to give reasonable agreement with the experimental results.

A.R.C. C.P. No. 883
January, 1965
Ackroyd, J. A. D.

A STUDY ON THE RUNNING TIMES IN REFLECTED SHOCK TUNNELS

The running time obtainable in a reflected shock tunnel is considered, particular attention being paid to the nature of the unsteady wave starting process in the nozzle. A range of initial conditions has been examined experimentally in a two-dimensional nozzle with a maximum efflux-to-throat area ratio of 100. An approximate analysis based on Chisnell's theory is shown to give reasonable agreement with the experimental results.

A.R.C. C.P. No. 883
January, 1965
Ackroyd, J. A. D.

A STUDY ON THE RUNNING TIMES IN REFLECTED SHOCK TUNNELS

The running time obtainable in a reflected shock tunnel is considered, particular attention being paid to the nature of the unsteady wave starting process in the nozzle. A range of initial conditions has been examined experimentally in a two-dimensional nozzle with a maximum efflux-to-throat area ratio of 100. An approximate analysis based on Chisnell's theory is shown to give reasonable agreement with the experimental results.

DETACHABLE ABSTRACT CARDS

Printed and published by

HER MAJESTY'S STATIONERY OFFICE

To be purchased from
49 High Holborn, London W C 1
423 Oxford Street, London W 1
13A Castle Street, Edinburgh 2
109 St Mary Street, Cardiff
Brazennose Street, Manchester 2
50 Fairfax Street, Bristol 1
35 Smallbrook, Ringway, Birmingham 5
80 Chichester Street, Belfast 1
or through any bookseller

Printed in England

S.O. Code No. 23-9016-83